



Ecological controls on N₂O emission in surface litter and near-surface soil of a managed grassland: modelling and measurements

Robert F. Grant¹, Albrecht Neftel², and Pierluigi Calanca²

¹Department of Renewable Resources, University of Alberta, Edmonton AB T6G 2E3, Canada

²Agroscope Institute for Sustainability Sciences ISS, Reckenholzstrasse 191, P.O.Box 8046, Zürich, Switzerland

Correspondence to: Robert F. Grant (rgrant@ualberta.ca)

Received: 2 December 2015 – Published in Biogeosciences Discuss.: 18 January 2016

Revised: 12 May 2016 – Accepted: 14 May 2016 – Published: 17 June 2016

Abstract. Large variability in N₂O emissions from managed grasslands may occur because most emissions originate in surface litter or near-surface soil where variability in soil water content (θ) and temperature (T_s) is greatest. To determine whether temporal variability in θ and T_s of surface litter and near-surface soil could explain this in N₂O emissions, a simulation experiment was conducted with *ecosys*, a comprehensive mathematical model of terrestrial ecosystems in which processes governing N₂O emissions were represented at high temporal and spatial resolution. Model performance was verified by comparing N₂O emissions, CO₂ and energy exchange, and θ and T_s modelled by *ecosys* with those measured by automated chambers, eddy covariance (EC) and soil sensors on an hourly timescale during several emission events from 2004 to 2009 in an intensively managed pasture at Oensingen, Switzerland. Both modelled and measured events were induced by precipitation following harvesting and subsequent fertilizing or manuring. These events were brief (2–5 days) with maximum N₂O effluxes that varied from $< 1 \text{ mg N m}^{-2} \text{ h}^{-1}$ in early spring and autumn to $> 3 \text{ mg N m}^{-2} \text{ h}^{-1}$ in summer. Only very small emissions were modelled or measured outside these events. In the model, emissions were generated almost entirely in surface litter or near-surface (0–2 cm) soil, at rates driven by N availability with fertilization vs. N uptake with grassland regrowth and by O₂ supply controlled by litter and soil wetting relative to O₂ demand from microbial respiration. In the model, NO_x availability relative to O₂ limitation governed both the reduction of more oxidized electron acceptors to N₂O and the reduction of N₂O to N₂, so that the magnitude of N₂O emissions was not simply related to surface and near-surface

θ and T_s . Modelled N₂O emissions were found to be sensitive to defoliation intensity and timing which controlled plant N uptake and soil θ and T_s prior to and during emission events. Reducing leaf area index (LAI) remaining after defoliation to half that under current practice and delaying harvesting by 5 days raised modelled N₂O emissions by as much as 80 % during subsequent events and by an average of 43 % annually. Modelled N₂O emissions were also found to be sensitive to surface soil properties. Increasing near-surface bulk density by 10 % raised N₂O emissions by as much as 100 % during emission events and by an average of 23 % annually. Relatively small spatial variation in management practices and soil surface properties could therefore cause the large spatial variation in N₂O emissions commonly found in field studies. The global warming potential from annual N₂O emissions in this intensively managed grassland largely offset those from net C uptake in both modelled and field experiments. However, model results indicated that this offset could be adversely affected by suboptimal land management and soil properties.

1 Introduction

The contribution of managed grasslands to reducing atmospheric greenhouse gas (GHG) concentrations through net uptake of CO₂ (Ammann et al., 2007) may be at least partially offset by net emissions of N₂O (Conant et al., 2005; Flécharde et al., 2005). These emissions may be substantial, with N₂O emission factors of as large as 3 % measured in

intensively managed grasslands with fertilizer rates of 25–30 g N m⁻² yr⁻¹ (Imer et al., 2013; Rafique et al., 2011). These emissions are highly variable temporally and spatially because they are determined by complex interactions among short-term weather events (warming, precipitation), land management practices (N amendments, defoliation) and soil properties (e.g. bulk density, water retention). The N₂O driving these emissions in managed grasslands is thought to be generated within the upper 2 cm of the soil profile (van der Weerden et al., 2013) and in surface litter left by grazing or harvesting (Pal et al., 2013) so that diurnal heating and precipitation events that cause rapid warming and wetting of the litter and soil surface may cause large but brief emission events. These events are thought to be driven by increased demand for electron acceptors by nitrification and denitrification, a reduced supply of O₂ by which these demands are preferentially met, and therefore increased demand for alternative acceptors NO₃⁻, NO₂⁻ and N₂O by autotrophic nitrifiers and heterotrophic denitrifiers.

The magnitude of N₂O emission events in managed grasslands generally increases with the amount of N added as urine, manure or fertilizer and with the intensity of defoliation by grazing or cutting (Ruzjerez et al., 1994). Thus, Imer et al. (2013) found a negative correlation between leaf area index (LAI) and N₂O emissions at intensively managed grasslands in Switzerland. The increase in emissions with defoliation has been attributed to increased urine and manure deposition and soil compaction with defoliation by grazing and to slower uptake of N and water by slower-growing plants with defoliation by harvesting (Jackson et al., 2015). Both N additions and defoliation are thought to raise these emissions by increasing the supply of NH₄⁺ and NO₃⁻ to autotrophic nitrifiers and heterotrophic denitrifiers. This increase raises the demand for alternative e⁻ acceptors by these microbial populations if the supply of O₂, the preferred e⁻ acceptor, fails to meet demand, as may occur when soil water content (θ) after defoliation rises with precipitation or reduced transpiration. This supply is governed by physical and hydrological properties (porosity, water retention) of the near-surface soil. Consequently, land use practices and soil properties must be considered when estimating N₂O emissions from managed grasslands.

Recognition of the effects of precipitation events, N amendments and soil properties on N₂O emissions has led to empirical models in which annual emission inventories are calculated directly from annual precipitation and N inputs (Lu et al., 2006) or in which monthly emission events are calculated from monthly precipitation, air temperature T_a , and θ (Flécharde et al., 2007). However, the soil depth at which most emitted N₂O is generated (0–2 cm) is much shallower than that at which θ used in these models is measured (5–10 cm) (Flécharde et al., 2007), and the soil temperature T_s at this depth may differ from T_a . This is particularly so for grasslands in which N additions are necessarily left on the

soil surface without incorporation. Thus, large N₂O emissions may be caused by surface wetting from precipitation on dry soils following fertilizer application, so that deeper θ is sometimes found to be of little explanatory value in empirical models (Flécharde et al., 2007). Furthermore, the response of denitrification to θ has been found in experimental studies to rise sharply with T_s , likely through the combined effects of T_s on increasing demand and reducing supply of O₂ at microbial microsites (Craswell, 1978). The interaction between T_s and θ on N₂O emissions is clearly apparent in the meta-analysis of N₂O emissions from European grasslands by Flécharde et al. (2007). This interaction has been represented in empirical models by fitting interdependent threshold values of T_s and θ above which emissions have been measured in field experiments (Smith and Massheder, 2014). However, a more robust simulation of this interaction with N₂O emissions should be built from basic biological and physical processes that are independent of site-specific measurements.

Process models used to simulate N₂O emissions from managed grasslands must therefore explicitly represent the effects of short-term weather events on near-surface T_s and θ , as well as the effects of N additions and defoliation on near-surface NH₄⁺ and NO₃⁻. These models must also explicitly represent the effects of mineral N, T_s and θ , and of soil physical and hydrological properties, on the demand for vs. supply of O₂ and alternative e⁻ acceptors NO₃⁻, NO₂⁻ and N₂O, and on the oxidation–reduction reactions by which these e⁻ acceptors are reduced. However, earlier process models have usually simulated N₂O emissions as T_s -dependent functions of nitrification and denitrification rates, modified by texture-dependent functions of water-filled pore space (WFPS) (e.g. Li et al., 2005). In some models additional empirical functions of T_s (Chatskikh et al., 2005), or of T_s and WFPS (Schmid et al., 2001), are used to calculate the fraction of nitrification that generates N₂O and the fraction of heterotrophic respiration R_h that drives denitrification (Schmid et al., 2001), thereby avoiding the explicit simulation of O₂ and its control on N₂O emissions. A more detailed summary of functions of the mineral N, T_s and WFPS currently used to model N₂O emissions is given in Fang et al. (2015). These functions have many model-dependent parameters and function independently of each other, so that key interactions among reduced C and N substrates, T_s and θ on N₂O production may not be simulated. In none of these approaches are the oxidation–reduction reactions by which N₂O is generated or consumed explicitly represented. Furthermore, the effects of defoliation and surface litter on N₂O emissions have not been considered in earlier process models.

Process models used to simulate N₂O emissions must also accurately represent the key processes of C cycling that drive those of N cycling, from which N₂O is generated and consumed. These include gross and net primary productivity (GPP and NPP), which drive mineral N uptake and assimilation.

lation with plant growth. GPP and consequent plant growth also drive autotrophic respiration (R_a), the below-ground component of which contributes to soil O₂ demand. NPP drives litterfall and root exudation, which in turn drive heterotrophic respiration (R_h) that also contributes to litter and soil O₂ demand and thereby to demand for alternative e⁻ acceptors which drive N₂O generation. Heterotrophic respiration also drives key N transformations such as mineralization or immobilization, thereby controlling availability of these alternative e⁻ acceptors. Land use practices, such as defoliation from grazing or harvesting, and soil properties, such as porosity and water retention, alter these key C cycling processes and thereby N₂O emissions. Therefore these emissions are best simulated by comprehensive ecosystem models.

In the mathematical model *ecosys*, the effects of weather and N amendments on T_s , θ and mineral N, and hence on the demand for vs. supply of O₂, NO₃⁻, NO₂⁻ and N₂O, and thereby on N₂O emissions, are simulated by explicitly coupling the transport processes with the oxidation–reduction reactions by which these e⁻ acceptors are known to be generated, transported and consumed in soils (Grant and Pattey, 1999, 2003, 2008; Grant et al., 2006; Metivier et al., 2009). The development of model algorithms for these processes was guided by two key principles:

1. all algorithms in the model must represent physical, biochemical and biological processes studied in basic research programs (e.g. convective–diffusive transport, oxidation–reduction reactions) so that these algorithms can be parameterized independently of the model;
2. this parameterization must be conducted on spatial and temporal scales smaller than those of prediction (in this case seasonal N₂O fluxes) so that site-specific effects on predicted values are not incorporated into the algorithms, limiting their robustness.

These principles are designed to avoid as much as possible the use of site- and model-specific algorithms that may lack application in sites and models other than those for which they were developed. Although models based on these principles appear complex, they can be better constrained than simpler models because they are parameterized from independent experiments. The resulting detail that the application of these principles brings to the model enables better-constrained tests of model output against more comprehensive and diverse site data than are possible with simpler models.

In an extension of earlier work with *ecosys*, we propose that temporal and spatial variation in N₂O emissions from an intensively managed grassland can be largely explained from the modelled effects of N amendments (fertilizer, manure), plant management (e.g. harvest intensity and timing), soil properties (e.g. bulk density) and weather (T_s , precipitation events) on the demand for vs. supply of O₂, NO₃⁻, NO₂⁻ and

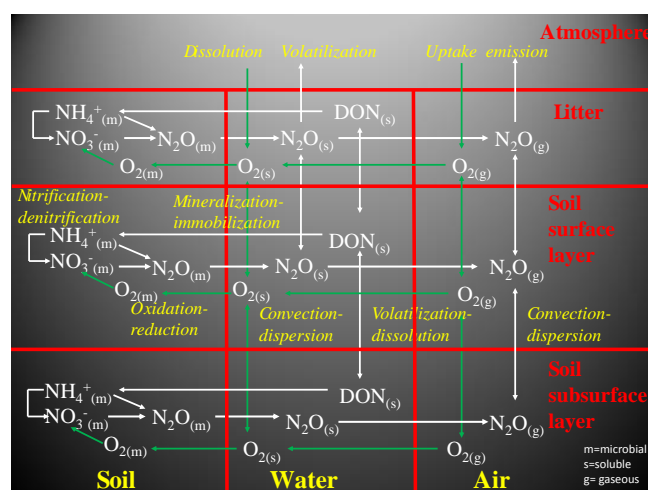


Figure 1. Summary of key processes governing generation and emission of N₂O as represented in *ecosys*.

N₂O in surface litter and near-surface soil (0–2 cm). Testing this explanation requires frequent measurements to characterize the large temporal variation in N₂O emissions found in managed ecosystems. Such measurements were recorded from 2004 to 2009 using automated chambers in intensively managed grass–clover grassland at Oensingen, Switzerland, and used here to test our modelled explanation of these fluxes.

2 Model development

2.1 General overview

The hypotheses for N₂O oxidation–reduction reactions and their coupling with gas transport in *ecosys* are represented in Fig. 1 and described further below with reference to equations and definitions listed in Sects. A, C, D, E and H of the Supplement (indicated by square brackets in the text below; e.g. [H1] refers to Eq. 1 in Sect. H), as well as in earlier papers (Grant and Pattey, 1999, 2003, 2008; Grant et al., 2006; Metivier et al., 2009). These hypotheses are part of a larger model of soil C, N and P transformations (Grant et al., 1993a, b), coupled to one of soil water, heat and solute transport in surface litter and soil layers, which are in turn components of the comprehensive ecosystem model *ecosys* (Grant, 2001).

2.2 Mineralization and immobilization of ammonium by all microbial populations

Heterotrophic microbial populations m (obligately aerobic bacteria, obligately aerobic fungi, facultatively anaerobic denitrifiers, anaerobic fermenters, acetotrophic methanogens, and obligately aerobic and anaerobic non-symbiotic diazotrophs) are associated with each organic

substrate i (i : animal manure, coarse woody plant residue, fine non-woody plant residue, particulate organic matter, or humus). Autotrophic microbial populations n (aerobic NH₄⁺ and NO₂⁻ oxidizers, hydrogenotrophic methanogens and methanotrophs) are associated with inorganic substrates. These populations grow with energy generated from the coupled oxidation of reduced dissolved organic C (DOC) by heterotrophs or of mineral N (NH₄⁺ and NO₂⁻) by nitrifiers and a reduction of e⁻ acceptors O₂ and NO_x. These populations decay according to first-order rate constants with provision for internal recycling of limiting nutrients (N, P). During growth, each functional component j (j : nonstructural, labile, resistant) of these populations seeks to maintain a set C:N ratio by mineralizing NH₄⁺ ([H1a]) from, or by immobilizing NH₄⁺ ([H1b]) or NO₃⁻ ([H1c]) to, microbial nonstructural N. Nitrogen limitations during growth may cause C:N ratios to rise above set values and a greater recovery of microbial N from structural to nonstructural forms to reduce N loss during decay but at a cost to microbial function. These transformations control the exchange of N between organic and inorganic states and hence affect the availability of alternative e⁻ acceptors for nitrification and denitrification.

2.3 Oxidation of DOC and reduction of oxygen by heterotrophs

Constraints on heterotrophic oxidation of DOC imposed by O₂ uptake are solved in four steps:

1. DOC oxidation under non-limiting O₂ is calculated from active biomass, DOC concentration and an Arrhenius function of T_s [H2];
2. O₂ reduction to H₂O under non-limiting O₂ (O₂ demand) is calculated from (1) using a set respiratory quotient [H3];
3. O₂ reduction to H₂O under ambient O₂ is calculated from radial O₂ diffusion through water films of thickness determined by soil water potential [H4a] coupled with active uptake at heterotroph surfaces driven by (2) [H4b]. O₂ diffusion and active uptake is calculated for each heterotrophic population associated with each organic substrate, allowing [H4] to calculate lower O₂ concentrations at microbial surfaces associated with more biologically active substrates (e.g. manure, litter). Localized zones of low O₂ concentration (hotspots) are thereby simulated when O₂ uptake by any aerobic population is constrained by O₂ diffusion to that population. O₂ uptake by each heterotrophic population also accounts for competition for O₂ uptake with other heterotrophs, nitrifiers, roots and mycorrhizae, calculated from its O₂ demand relative to those of other aerobic populations;

4. DOC oxidation to CO₂ under ambient O₂ is calculated from (2) and (3) [H5]. The energy yield of DOC oxidation drives the uptake of additional DOC for the construction of microbial biomass $M_{i,h}$ according to construction energy costs of each heterotrophic population [A21]. Energy costs of denitrifiers are larger than those of obligately aerobic heterotrophs, placing denitrifiers at a competitive disadvantage for growth and hence DOC oxidation that declines with greater use of e⁻ acceptors other than O₂.

2.4 Oxidation of DOC and reduction of nitrate, nitrite and nitrous oxide by denitrifiers

Constraints imposed by NO₃⁻ availability on DOC oxidation by denitrifiers are solved in five steps:

1. NO₃⁻ reduction to NO₂⁻ under non-limiting NO₃⁻ is calculated from electrons demanded by DOC oxidation to CO₂ but not met by O₂ reduction to H₂O because of diffusion limitations to O₂ supply, and hence transferred to NO₃⁻ [H6];
2. NO₃⁻ reduction to NO₂⁻ under ambient NO₃⁻ is calculated from (1), accounting for relative concentrations and affinities of NO₃⁻ and NO₂⁻ [H7];
3. NO₂⁻ reduction to N₂O under ambient NO₂⁻ is calculated from demand for electrons not met by NO₃⁻ reduction in (2), accounting for relative concentrations and affinities of NO₂⁻ and N₂O [H8];
4. N₂O reduction to N₂ under ambient N₂O is calculated from demand for electrons not met by NO₂⁻ reduction in (3) [H9];
5. additional DOC oxidation to CO₂ enabled by NO_x reduction in (2), (3) and (4) is added to that enabled by O₂ reduction from [H5], the energy yield of which drives additional DOC uptake for the construction of $M_{i,n}$. This additional uptake offsets the disadvantage incurred by the larger construction energy costs of denitrifiers.

2.5 Oxidation of ammonia and reduction of oxygen by nitrifiers

Constraints on nitrifier oxidation of NH₃ imposed by O₂ uptake are solved in four steps:

1. substrate (NH₃) oxidation under non-limiting O₂ is calculated from active biomass, NH₃ and CO₂ concentrations and an Arrhenius function of T_s [H11];
2. O₂ reduction to H₂O under non-limiting O₂ is calculated from (1) using set respiratory quotients [H12];
3. O₂ reduction to H₂O under ambient O₂ is calculated from radial O₂ diffusion through water films of thick-

ness determined by soil water potential [H13a] coupled with active uptake at nitrifier surfaces driven by (2) [H13b]. O₂ uptake by nitrifiers also accounts for competition for O₂ uptake with heterotrophic DOC oxidizers, roots and mycorrhizae;

- NH₃ oxidation to NO₂⁻ under ambient O₂ is calculated from (2) and (3) [H14]. The energy yield of NH₃ oxidation drives the fixation of CO₂ for the construction of microbial biomass $M_{i,n}$ according to construction energy costs of nitrifier populations.

2.6 Oxidation of nitrite and reduction of oxygen by nitrifiers

Constraints on nitrifier oxidation of NO₂⁻ to NO₃⁻ imposed by O₂ uptake [H15–H18] are solved in the same way as are those of NH₃ [H11–H14]. The energy yield of NO₂⁻ oxidation drives the fixation of CO₂ for construction of microbial biomass $M_{i,o}$ according to the construction energy costs of each nitrifier population.

2.7 Oxidation of ammonia and reduction of nitrite by nitrifiers

Constraints on nitrifier oxidation of NH₃ imposed by NO₂⁻ availability are solved in three steps:

- NO₂⁻ reduction to N₂O under non-limiting NO₂⁻ is calculated from electrons demanded by NH₃ oxidation but not accepted for O₂ reduction to H₂O because of diffusion limitations to O₂ supply and hence transferred to NO₂⁻ [H19];
- NO₂⁻ reduction to N₂O under ambient NO₂⁻ and CO₂ is calculated from (1) [H20], competing for NO₂⁻ with denitrifiers [H8] and nitrifiers [H18];
- additional NH₃ oxidation to NO₂⁻ enabled by NO₂⁻ reduction in (2) [H21] is added to that enabled by O₂ reduction from [H14]. The energy yield from this oxidation drives the fixation of additional CO₂ for the construction of $M_{i,n}$.

2.8 Uptake of ammonium and reduction of oxygen by roots and mycorrhizae

- NH₄⁺ uptake by roots and mycorrhizae under non-limiting O₂ is calculated from mass flow and radial diffusion between adjacent roots and mycorrhizae [C23a] coupled with active uptake at root and mycorrhizal surfaces [C23b]. Active uptake is subject to inhibition by root nonstructural N : C ratios [C23g], where nonstructural N is the active uptake product and nonstructural C is the CO₂ fixation product transferred to roots and mycorrhizae from the canopy.

- O₂ reduction to H₂O is calculated from (1) plus oxidation of root and mycorrhizal nonstructural C under non-limiting O₂ using a set respiratory quotient [C14e].
- O₂ reduction to H₂O under ambient O₂ is calculated from mass flow and radial diffusion between adjacent roots and mycorrhizae [C14d] coupled with active uptake at root and mycorrhizal surfaces driven by (2) [C14c]. O₂ uptake by roots and mycorrhizae also accounts for competition with O₂ uptake by heterotrophic DOC oxidizers and autotrophic nitrifiers calculated from their O₂ demands relative to those of other populations.
- Oxidation of root and mycorrhizal nonstructural C to CO₂ under ambient O₂ is calculated from (2) and (3) [C14b].
- NH₄⁺ uptake by roots and mycorrhizae under ambient O₂ is calculated from (1), (2), (3) and (4) [C23b].

2.9 Cation exchange and ion pairing of ammonium

A Gapon selectivity coefficient is used to solve cation exchange of NH₄⁺ vs. Ca²⁺ [E10] as affected by other cations [E11]–[E15] and CEC (cation exchange capacity) [E16]. A solubility product is used to equilibrate soluble NH₄⁺ and NH₃ [E24] as affected by pH [E25] and other solutes [E26–E57].

2.10 Soil transport and surface – atmosphere exchange of gaseous substrates and products

Exchange of all modelled gases γ ($\gamma = \text{O}_2, \text{CO}_2, \text{CH}_4, \text{N}_2, \text{N}_2\text{O}, \text{NH}_3$ and H₂) between aqueous and gaseous states is driven by disequilibrium between aqueous and gaseous concentrations according to a T_s -dependent solubility coefficient, constrained by a transfer coefficient based on an air–water interfacial area that depends on air-filled porosity [D14–D15] (Fig. 1). These gases undergo convective–dispersive transport through soil in gaseous [D16] and aqueous [D19] states driven by soil water flux and by gas concentration gradients. Dispersive transport is controlled by gaseous diffusion [D17] and aqueous dispersion [D20] coefficients calculated from gas- and water-filled porosity. Exchange of all gases between the atmosphere and both gaseous and aqueous states at the soil surface are driven by atmosphere–surface gas concentration differences and by boundary layer conductance above the soil surface, calculated from wind speed and from the structure of vegetation and surface litter [D15].

Table 1. Key soil properties of the Eutri-Stagnic Cambisol at Oensingen as used in *ecosys*.

Depth (m)	BD ^a (Mg m ⁻³)	TOC		FC ^b		K _{sat} ^b (mm h ⁻¹)	pH	Sand ^a			CF (m ³ m ⁻³)
		TON	(g kg ⁻¹)	WP ^b	(m ³ m ⁻³)			Silt ^a	Clay ^a	(g kg ⁻¹)	
0.01	1.21	27.2	2.9	0.38	0.22	3.4	7	240	330	430	0
0.03	1.21	27.2	2.9	0.38	0.22	3.4	7	240	330	430	0
0.07	1.21	27.2	2.9	0.38	0.22	3.4	7	240	330	430	0
0.13	1.24	27.2	2.9	0.39	0.23	3.4	7	240	330	430	0
0.28	1.28	20.2	2.1	0.40	0.24	2.4	7	180	380	440	0
0.6	1.28	11.6	1.1	0.40	0.24	1.4	7	180	380	440	0
0.7	1.28	11.6	1.1	0.40	0.24	1.4	7	180	380	440	0
0.9	1.28	9	0.9	0.40	0.24	1.4	7	180	380	440	0
1.5	1.28	6	0.6	0.40	0.24	1.4	7	180	380	440	0.1

Abbreviations: BD: bulk density; TOC: total organic C; TON: total organic N; FC: field capacity; WP: wilting point; K_{sat}: saturated hydraulic conductivity; CF: coarse fragments.

^a BD, TOC and texture were determined from soil cores taken in 2001 and 2006. Details are given in Leifeld et al. (2011).

^b FC, WP and K_{sat} were estimated from BD, TOC and texture according to Saxton et al. (1996) and Saxton and Rawls (2006).

3 Field experiment

3.1 Site description

The Oensingen field site is located in the central Swiss lowlands (7°44' E, 47°17' N) at an altitude of 450 m. The climate is temperate with an average annual rainfall of about 1100 mm and a mean air temperature of 9.5 °C. The soil is classified as a Eutri-Stagnic Cambisol developed on clayey alluvial deposits, key properties of which are given in Table 1. Prior to the experiment, the field site was managed as a ley–arable rotation. In December 2000, the field was ploughed and left in fallow until 11 May 2001. The field was then sown with a grass–clover mixture typical for permanent grassland under intensive management. The field was ploughed again on 19 December 2007, left in fallow until 5 May 2008, when it was tilled and resown with the same grass–clover mix as in 2001. The period of study extended from sowing in 2001 to the end of 2009, during which the field was cut between three and five times per year and harvested as hay, silage or fresh grass; it was fertilized two to three times per year with manure as liquid cattle slurry and two to three times per year with mineral fertilizer as ammonium nitrate (NH₄NO₃) pellets, for an average annual N application of 23 g N m⁻². All key management operations during this period are summarized in Table 2.

3.2 Soil, plant and meteorological measurements

Soil θ and T_s were recorded continuously using TDR (time domain reflectometry, ThetaProbe ML2x, Delta-T Devices, Cambridge, UK) and thermocouples at 5, 10, 30 and 50 cm for θ and at 2, 5, 10, 30 and 50 cm for T_s . Leaf area index (LAI) was measured weekly with an optical leaf area meter (LI-2000, Li-Cor, Lincoln, NB, USA). Plants were collected every 2–4 weeks, and the samples were dried for 48 h at 80 °C and weighed and analysed for C, N, P and K by using

an elemental analyzer. Hourly climatic data were recorded continuously with an automated meteorological station, including air temperature (°C), rainfall (mm), relative humidity (%), global radiation (W m⁻²) and wind speed (m s⁻¹).

3.3 Nitrous oxide flux measurements

N₂O fluxes were measured with a fully automated system consisting of up to eight stainless steel chambers (30 cm × 30 cm × 25 cm) (Flécharde et al., 2005; Felber et al., 2014) fixed on PVC frames permanently inserted 10 cm deep into the soil. The positions of the chambers were changed about every 2 months. During measurements, the lids of the chambers were sequentially closed for 15 min every 2 h to allow N₂O accumulation in the chamber headspace. During closure the chamber atmosphere was recirculated at a rate of 1000 mL min⁻¹ through polyamide tube lines (4 mm ID) to analytical instruments installed in a temperature-controlled field cabin adjacent to the field plots (10 m) and then back to the chamber headspace. Until autumn 2006, concentrations of N₂O, CO₂ and H₂O in the head space were measured once per minute with an INNOVA 1312 photoacoustic multi-gas analyzer (INNOVA Air Tech Instruments, Ballerup, Denmark; www.innova.dk). Interferences in the measurements caused by overlaps in the absorption spectra of the different gases and by temperature effects were corrected with a calibration algorithm described in detail by Flécharde et al. (2005). In autumn 2006, the system was changed to the gas filter correlation technique for N₂O (Model 46C, Thermo 279 Environmental Instruments Inc., Sunnyvale, CA, USA). This system was calibrated every 8 hours using certified standard gas mixtures (Messer Schweiz AG, Lenzburg, Switzerland) (Felber et al., 2014).

These measurements were used to calculate N₂O fluxes from the rate of change in concentration by using a linear or non-linear approach determined by the HMR R-package

Table 2. Plant and soil management operations at the Oensingen intensively managed grassland from 2001 to 2009.

Year	Plant management		Soil management					
	Date	Management	Date	Management	Amount (g m ⁻²)			
					NH ₄ ⁺	NO ₃ ⁻	ON	OC
2001			7 May	tillage				
			10 May	tillage				
	11 May	planting	15 Jun	mineral fertilizer	1.5	1.5		
	1 Jul	harvest	12 Jul	mineral fertilizer	1.5	1.5		
	8 Aug	harvest	16 Aug	mineral fertilizer	1.15	1.15		
	12 Sep	harvest						
	31 Oct	harvest						
2002			12 Mar	mineral fertilizer	1.5	1.5		
	15 May	harvest	22 May	manure slurry	4.2		2.8	31.2
	25 Jun	harvest	1 Jul	mineral fertilizer	1.75	1.75		
	15 Aug	harvest	18 Aug	manure slurry	5.9		5.3	49.6
	18 Sep	harvest	30 Sep	mineral fertilizer	1.5	1.5		
	7 Dec	harvest						
2003			18 Mar	manure slurry	5.9		5.3	61.1
	30 May	harvest	2 Jun	mineral fertilizer	1.5	1.5		
	4 Aug	harvest	18 Aug	manure slurry	6.3		1.9	19.0
	13 Oct	harvest						
2004			17 Mar	manure slurry	5.0		1.5	19.5
	11 May	harvest	17 May	mineral fertilizer	1.5	1.5		
	25 Jun	harvest	1 Jul	manure slurry	5.5		0.5	9.9
	28 Aug	harvest	31 Aug	mineral fertilizer	1.5	1.5		
	3 Nov	harvest						
2005			29 Mar	manure slurry	6.7		3.1	42.0
	10 May	harvest	17 May	mineral fertilizer	1.5	1.5		
	27 Jun	harvest	5 Jul	manure slurry	5.0		3.5	59.6
	29 Aug	harvest	16 Sep	mineral fertilizer	1.5	1.5		
	24 Oct	harvest						
2006	24 May	harvest						
	5 Jul	harvest	13 Jul	manure slurry	4.7		1.4	12.5
	12 Sep	harvest	27 Sep	manure slurry	4.4		1.3	13.6
	26 Oct	harvest	30 Oct	manure slurry	6.4		3.2	57.8
2007			3 Apr	manure slurry	5.2		4.6	75.1
	26 Apr	harvest	3 May	mineral fertilizer	1.5	1.5		
	6 Jul	harvest	13 Jul	manure slurry	4.9		1.8	45.9
	23 Aug	harvest	28 Aug	mineral fertilizer	1.5	1.5		
	11 Oct	harvest	24 Oct	manure slurry	4.6		3.0	38.9
	19 Dec	terminate	19 Dec	plowing				
2008			1 May	tillage				
			4 May	tillage				
	5 May	planting						
	1 Jul	harvest	10 Jul	mineral fertilizer	1.5	1.5		
	29 Jul	harvest	7 Aug	mineral fertilizer	1.5	1.5		
	8 Sep	harvest	19 Sep	manure slurry	2.9		0.5	8.6
	7 Nov	harvest						
2009			7 Apr	mineral fertilizer	1.5	1.5		
	1 May	harvest	12 May	manure slurry	4.4		1.6	26.0
	16 Jun	harvest	6 Aug	manure slurry	3.3		1.2	19.0
	29 Jul	harvest						
	7 Sep	harvest	15 Sep	mineral fertilizer	6.5 (urea)			
	20 Oct	harvest						

(Pedersen et al., 2010). The first three of the fifteen 1 min measurements were omitted from the flux calculation to exclude gas exchange during closing that did not result from changes in emission or production in the soil. This procedure caused a mean increase of about 30 % in the fluxes compared to values published in Flécharde et al. (2005) and Ammann et al. (2009), which were evaluated using linear regression. Fluxes from all chambers were averaged over 4-hourly intervals and resulting values attributed to the mid-points of the intervals. Standard errors of these averages were calculated from all fluxes measured during each interval and thus included both spatial and temporal variation. The fluxes measured from 2002 to 2003 were summarized in Flécharde et al. (2005). Those from 2004 to 2007 were re-evaluated from values described in Ammann et al. (2009). Those from 2008 and 2009 were reprocessed from the EU Project NitroEurope-IP database using the HMR algorithm.

3.4 CO₂ and energy flux measurements

CO₂ and energy fluxes were measured by an eddy covariance (EC) system consisting of three-axis sonic anemometers (models R2 and HS, Gill instruments, Lymington, UK) and an open-path infrared CO₂/H₂O gas analyzer (model LI-7500, Li-Cor, Lincoln, USA). The EC system used in this study is described in Ammann et al. (2007). The EC tower was located in the centre of the field (52 m × 146 m), whereas the chambers were located in the south-east corner. For most meteorological conditions, the chambers were not within the footprint of the EC towers, although for the main wind directions 80 % or more of the footprint was within the field (Neftel et al., 2008). The management of the entire field was uniform throughout the experiment.

4 Model experiment

Ecosys was initialized with the biological properties of plant functional types (PFTs) representing the ryegrass and clover planted at Oensingen. These properties were identical to those in an earlier study (Grant et al., 2012) except for a perennial rather than annual growth habit. These PFTs competed for common resources of radiation, water and nutrients, based on their vertical distributions of leaf area and root length driven by uptake and allocation of C, N and P in each PFT. *Ecosys* was also initialized with the physical and chemical properties of the Eutri-Stagnic Cambisol at Oensingen (Table 1). The model was then run from model dates 1 January 1931–31 December 2000 under repeating sequences of land management practices and continuous hourly weather data (radiation, T_a , RH, wind speed and precipitation) recorded at Oensingen from 1 January 2001 to 31 December 2007 (i.e. 10 cycles of 7 years). This run was long enough for C, N and energy cycles in the model to attain equilibrium under the Oensingen site conditions well before

the end of the spinup run. The modelled site was plowed on 19 December 2000, terminating all PFTs.

The model run was then continued from model dates 1 January 2001 to 31 December 2009 under continuous hourly weather data recorded at Oensingen from 1 January 2001 to 31 December 2009 with the same PFTs and land management practices as those at the field site listed in Table 2. For each manure application in the model, an irrigation of 4 mm was added to account for the water in the slurry. For each harvest in the model, the fraction of canopy LAI to be cut (usually 0.85–0.95) was calculated from measurements of LAI before and after the corresponding harvest in the field. In *ecosys*, leaves of each PFT are aggregated into a common canopy which is dynamically resolved into a selected number of layers (10 in this case) of equal LAI for calculating irradiance interception. The leaf fraction to be cut was removed from successive leaf layers from the top of the combined canopy downwards until the cumulative removal attained the set fraction, so that the LAI cut from each PFT depended on the leaf area of the PFT in these layers. Of the phytomass cut with the LAI, 0.76 was removed as harvest and the remainder was added to surface litter, as determined in the intensively managed grassland at Oensingen by Ammann et al. (2009). N₂O emissions modelled from 2004 through 2009 were compared with those measured by the automated chambers by regressing log-transformed 4 h averages of modelled on measured values during each year of the study and also by regressing total emissions modelled vs. measured during emission events following each fertilizer or manure application. These comparisons were supported by ones with thermistor and TDR measurements of T_s and θ and with EC measurements of CO₂ and energy exchange.

Model sensitivity studies

Modelled N₂O emissions may be affected by three general sources of uncertainty in model inputs: land management practices, soil properties and model parameters. To examine the possible effects of some different land management practices on N₂O emissions, the model run from 2001 to 2009 (field) was repeated with (1) increased harvest intensity, in which canopy LAI remaining after each harvest was reduced to half of that in the first run (1/2), and (2) increased harvest intensity with each harvest delayed by 5 days (1/2 + 5 d). These alternative practices caused canopy regrowth and hence N uptake to be slower during emission events following subsequent manure and fertilizer applications.

To examine the possible effects of spatial variability in soil properties on N₂O emissions, the model run from 2001 to 2009 (field) was repeated with bulk density (BD) of the upper 3 cm in the soil profile (Table 1) increased by 5 or 10 %. These larger BDs reduced soil porosity in the upper 3 cm of the soil, thereby slowing gas exchange with the atmosphere,

particularly when the soil was wet (Fig. 1). All other soil properties used in the model remained unchanged (Table 1).

To examine an effect of uncertainty in model parameterization, the model run from 2001 to 2009 (field) was repeated with the values of two key parameters governing N₂O emissions, the Michaelis–Menten constants for the reduction of O₂ (K_{O_2} in [H4]) or of NO₃⁻ and NO₂⁻ (K_{NO_x} in [H7], [H8] and [H20]), halved or doubled from those used in the model. Halving or doubling K_{O_2} hastened or slowed the reduction of O₂ by nitrifiers and denitrifiers and hence slowed or hastened the transfer of electrons to reduce NO₂⁻ and NO₃⁻ during nitrification and denitrification. Halving or doubling K_{NO_x} hastened or slowed the reduction of NO₂⁻ by nitrifiers and of NO₃⁻ and NO₂⁻ by denitrifiers. All other parameters in the model remained unchanged.

5 Results

5.1 LAI modelled vs. measured from 2002 to 2009

Accurate modelling of ecosystem C cycling and hence N₂O emissions requires accurate modelling of plant growth as determined by land management practices. LAI modelled and measured from 2002 to 2009 rose rapidly from low values remaining in spring and after each harvest (Table 1) to 4–6 m² m⁻² before the next harvest, except during 2003 (Fig. 2). Regrowth of LAI in *ecosys* was driven by plant non-structural C, N and P pools replenished from storage reserves remobilized after harvests and from products of current C, N and P uptake, those of C being governed by irradiance interception calculated from regrowing LAI. Regrowth in the model was less rapid than that measured in 2009 (Fig. 2) because more frequent cutting forced more frequent replenishment of plant nonstructural C, N and P pools, which gradually depleted storage reserves and hence slowed subsequent regrowth. Hence, rates of regrowth modelled after harvests were affected by harvest timing and intensity, as represented by the fractions of LAI removed at harvest.

5.2 N₂O fluxes modelled vs. measured from 2004 to 2009

During peak emissions, standard deviations of N₂O fluxes measured within each 4-hourly interval were found to be as much as 85 % relative to mean values. These deviations were largely attributed to small-scale spatial variation in land management (manure and fertilizer application, surface litter from harvesting) and in soil properties (bulk density, water retention), which was not represented in the model run, rather than to temporal variation in environmental conditions (θ , T_s), which was represented in the model run. Therefore, only a limited fraction of variation in the measured values was amenable to correlation with modelled values. Consequently, slopes and coefficients of determination (R^2) from regressions of modelled on measured log-transformed fluxes

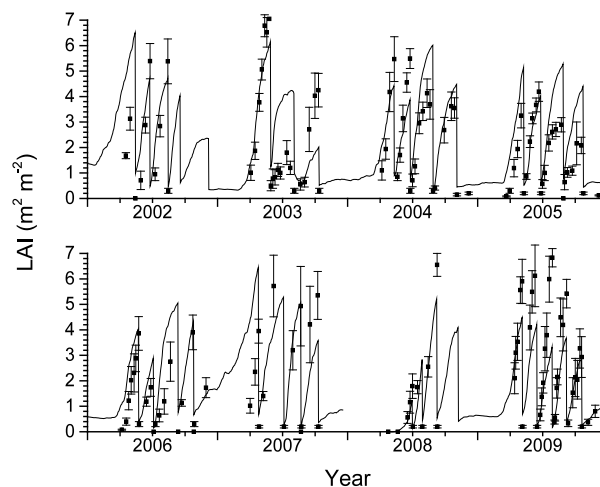


Figure 2. LAI measured (symbols) and modelled (lines) from 2002 through 2009 at the Oensingen intensively managed grassland.

varied from 0.5 to 1.0 and from 0.1 to 0.5 respectively, while intercepts remained close to zero (Table 3a). However, ratios of mean squares for regression vs. error (F) were highly significant ($P < 0.001$) in all years of the study, indicating some agreement in the timing and magnitude of modelled and measured emission events. Improved agreement would require that more detailed information about land management and soil properties at each chamber site be provided to the model.

5.3 Daily aggregated N₂O fluxes modelled vs. measured from 2004 to 2009

Daily aggregations of both measured and modelled N₂O emissions indicated that emission events during the study period were confined to intervals of no longer than 5 days when precipitation followed manure or fertilizer applications (Fig. 3). Outside of these intervals emissions remained very small except for a period of emissions modelled but not measured after manure application in autumn 2006 (Fig. 3c) and measured but not modelled before fertilizer application in spring 2008 (Fig. 3e).

The largest emissions followed manure applications in July and August, but their magnitudes did not vary with the amount of manure N applied. For example, emissions during an event in August 2009 (244 vs. 185 mg N m⁻² measured vs. modelled in Fig. 3f) were greater than those during an event in July 2007 (86 vs. 112 mg N m⁻² measured vs. modelled in Fig. 3d), which in turn were greater than those during an event in July 2005 (54 vs. 96 mg N m⁻² measured vs. modelled in Fig. 2b). However, manure N application preceding the event in August 2009 (4.5 g N m⁻²) was less than that in July 2007 (6.7 g N m⁻²), which in turn was less than that in July 2005 (8.5 g N m⁻²) (Table 2), so that smaller ap-

Table 3. Intercepts (*a*), slopes (*b*), coefficients of determination (*R*²), ratios of mean squares for regression vs. error (*F*), and number of data pairs from regressions of (a) log-transformed 4 h averages of N₂O fluxes (mg N m⁻² h⁻¹) modelled vs. measured during each year from 2004 to 2009 and (b) total N₂O fluxes (mg N m⁻²) modelled vs. measured during emission events following each fertilizer or manure application from 2004 to 2009 (see Fig. 3) at the Oensingen intensively managed grassland.

	Year	<i>a</i>	<i>b</i>	<i>R</i> ²	<i>F</i> *	<i>n</i>
(a)	2004	1.25 ± 0.88 × 10 ⁻⁵	0.49 ± 0.06	0.08	69	818
	2005	1.63 ± 0.43 × 10 ⁻⁵	0.59 ± 0.03	0.24	368	1173
	2006	4.28 ± 0.44 × 10 ⁻⁵	1.04 ± 0.08	0.14	155	948
	2007	1.21 ± 0.33 × 10 ⁻⁵	0.67 ± 0.02	0.35	989	1794
	2008	1.44 ± 0.51 × 10 ⁻⁵	0.44 ± 0.03	0.08	157	1703
	2009	-0.03 ± 0.25 × 10 ⁻⁵	0.71 ± 0.02	0.49	1574	1614
(b)	2004–2009	28 ± 9 mg N m ⁻²	0.67 ± 0.13	0.54	27	23

* All values of *F* were highly significant (*P* < 0.001).

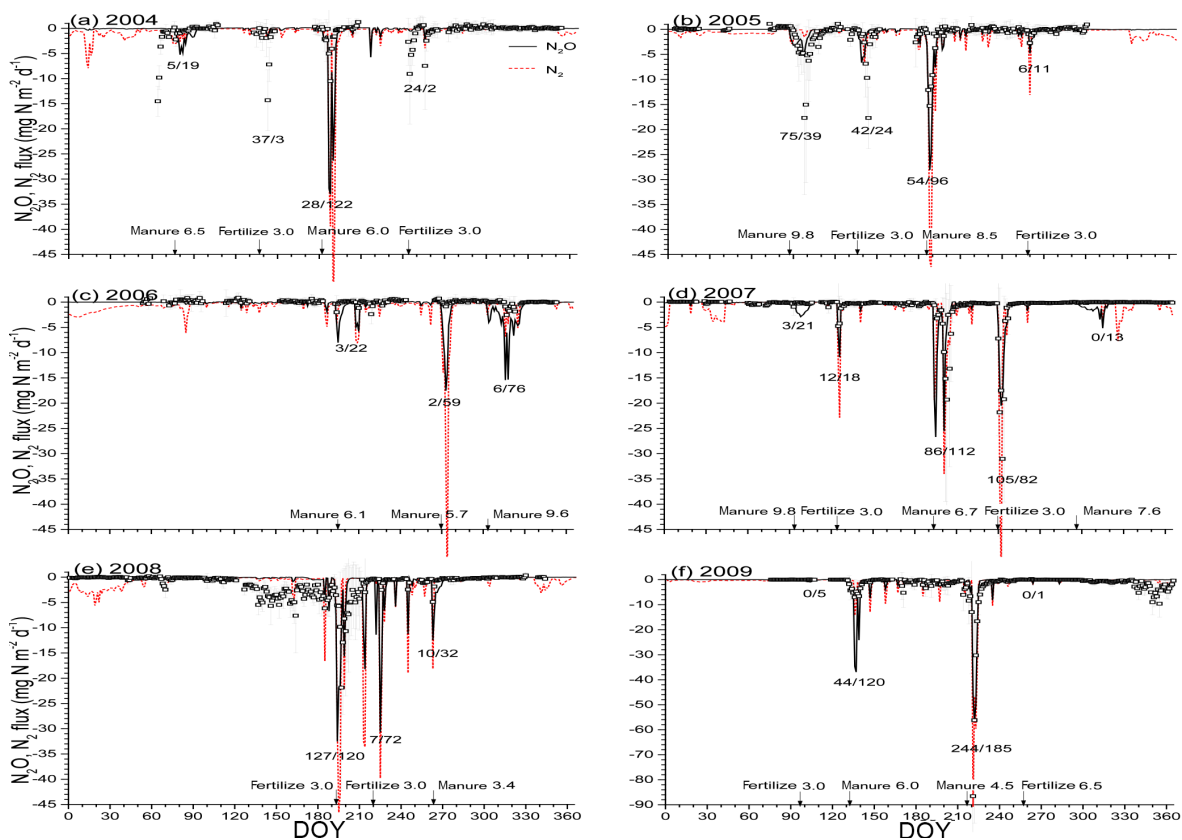


Figure 3. Daily aggregated N₂O emissions measured (symbols) and N₂O and N₂ emissions modelled (lines) from 2004 through 2009 at the Oensingen intensively managed grassland. Numbers above and beside each fertilizer or manure addition indicate total measured or modelled N₂O-N emitted during emission events (mg N m⁻²) and total N applied (g N m⁻²). Negative values indicate effluxes to the atmosphere.

plications were followed by greater emissions, precluding a simple emission factor for manure N application.

The magnitude of emission events following fertilizer application also varied. For example, emissions during an event in late August 2007 (105 vs. 82 mg N m⁻² measured vs. modelled in Fig. 3d) were greater than those during events in

September 2004 (24 vs. 2 mg N m⁻² measured vs. modelled in Fig 2a) and 2005 (6 vs. 11 mg N m⁻² measured vs. modelled in Fig. 3b), although the fertilizer N applications of 3.0 g N m⁻² preceding each event were the same (Table 2). These differences in emissions indicated important differ-

ences in ecological controls imposed by environmental conditions (θ and T_s) and plant management during each event.

The standard deviations of $\sim 85\%$ relative to the mean values of fluxes measured within each 4-hourly interval during emission events was used to estimate an uncertainty in daily aggregated fluxes of ca. 30%. Uncertainty in daily fluxes measured during emission events was smaller than the severalfold differences among the events indicating that the magnitude of these events likely differed significantly. Regressions of modelled on measured total emissions during the events following each fertilizer or manure application from 2004 to 2009 (Fig. 3) gave better agreement than did those of the 4-hourly averaged fluxes (Table 3b), indicating that modelling the precise timing of fluxes during these events remains a challenge.

5.4 Relationships between N₂O fluxes and environmental conditions during selected emission events

Environmental conditions measured and modelled from harvest to the end of the two largest emission events following manure applications in July 2007 (Fig. 3d) and August 2009 (Fig. 3f) were examined in greater detail to investigate relationships among near-surface T_s , θ , aqueous gas concentrations, and surface fluxes of energy, CO₂ and N₂O (Figs. 4, 5). In July 2007, several small precipitation events wetted and cooled the soil between harvesting on DOY 187 and manure application on DOY 194 (Fig. 4a, b). The soil then dried during several days without precipitation and warmed with reduced shading from defoliation (Fig. 2) until DOY 200, after which the soil wetted with further precipitation and cooled with increased shading from plant regrowth (Fig. 4a, b). The higher θ measured during this period (Fig. 4b) may have been caused by difficulties in maintaining the calibration of the TDR probes over long periods in the high-clay soil at Oensingen (Table 1). This higher θ was not likely caused by overestimated evapotranspiration because modelled latent heat (LE) fluxes, reduced by low LAI after harvesting but increasing with subsequent regrowth, were close to those measured (Fig. 4c), suggesting that total water uptake was accurately modelled. Comparison of modelled and measured θ was further complicated by soil cracking which altered infiltration at low θ . The effects of θ -dependent macroporosity on preferential flow are explicitly modelled in *ecosys* but have not yet been tested in detail.

CO₂ influxes were also reduced by low LAI after cutting but recovered to pre-cut levels by the end of the emission event (Fig. 4d), driving rapid regrowth of LAI (Fig. 2). Large CO₂ effluxes measured and modelled after manure application indicated rapid R_h and hence O₂ demand that persisted for several days. Influxes measured in the field were reduced from those in the model for several days after manure application, suggesting temporary interference of CO₂ fixation by

the manure application which was not accounted for in the model.

Litterfall from plant growth [C18, C19] and cutting as well as from manure application caused a litter layer of 1–2 cm to develop on the soil surface in the model. During the N₂O emission event from DOY 200 to DOY 205 in 2007 (Fig. 3d), several precipitation events (Fig. 4a) wetted the modelled surface litter and near-surface soil (layers 1 and 2 in Table 1) (Fig. 4e) without increasing θ at 5 cm (Fig. 4b). This surface wetting slowed gas exchange with the atmosphere, sharply reducing aqueous O₂ concentrations [O_{2(s)}] (Fig. 4f) and thereby raising aqueous N₂O concentrations [N₂O_(s)] (Fig. 4g). Between precipitation events, drying of the surface litter and near-surface soil in the model allowed the recovery of [O_{2(s)}] and forced declines in [N₂O_(s)]. These rises and declines in [N₂O_(s)] drove rises and declines in N₂O emissions that tracked those measured in the chambers (Fig. 4h). These emissions rose immediately with the onset of precipitation on DOY 200 (Fig. 4a) before wetting occurred at 5 cm (Fig. 4b), indicating that emissions were driven by surface wetting (Fig. 4e) combined with rapid O₂ demand (Fig. 4d). The net generation of N₂O modelled in each soil zone, calculated from [H8] + [H20] – [H9], indicated that 0.21 of surface emissions originated in the surface litter and the remainder in the 0–1 cm soil layer as indicated by higher [N₂O_(s)] (Fig. 4g), while the deeper soil layers were a very small net sink of N₂O. Rises and declines in [N₂O_(s)] also drove rises and declines in N₂ emissions that persisted until DOY 205, after which more rapid mineral N uptake with recovering plant growth, driven by rising LAI (Fig. 2) and hence CO₂ influxes (Fig. 4d), caused both emissions to return to background levels (Fig. 4h).

In 2009, a period of low precipitation with soil drying and warming occurred between harvesting in late July and manure application on DOY 218 in early August, followed by heavy precipitation with soil wetting and cooling on DOY 220 (Fig. 5a, b). LE effluxes and CO₂ influxes declined sharply with LAI after cutting, and did not recover to pre-cut levels by the end of the subsequent emission event on DOY 224 (Fig. 5c, d), indicating a slow recovery of plant growth. Slurry application caused brief surface wetting on DOY 218 (Fig. 5e) and heavy precipitation on DOY 220 caused prolonged soil wetting at the surface (Fig. 5e) and at 5 cm (Fig. 5b). Wetting caused declines in [O_{2(s)}] (Fig. 5f) and thereby rises in [N₂O_(s)] (Fig. 5g) that were sustained over 3 days. These rises drove particularly rapid N₂O emissions in the model which were consistent in magnitude with those measured in the chambers (Fig. 5h). Diurnal variation modelled with soil warming and cooling (Fig. 5a) was not apparent in the measurements, although modelled values remained within the large uncertainty of the measured values during the emission event. These large emissions were enabled in the model by slow plant uptake of manure N (Table 2) caused by the slow recovery of plant CO₂ uptake and hence growth after cutting (Fig. 5d). The rises in

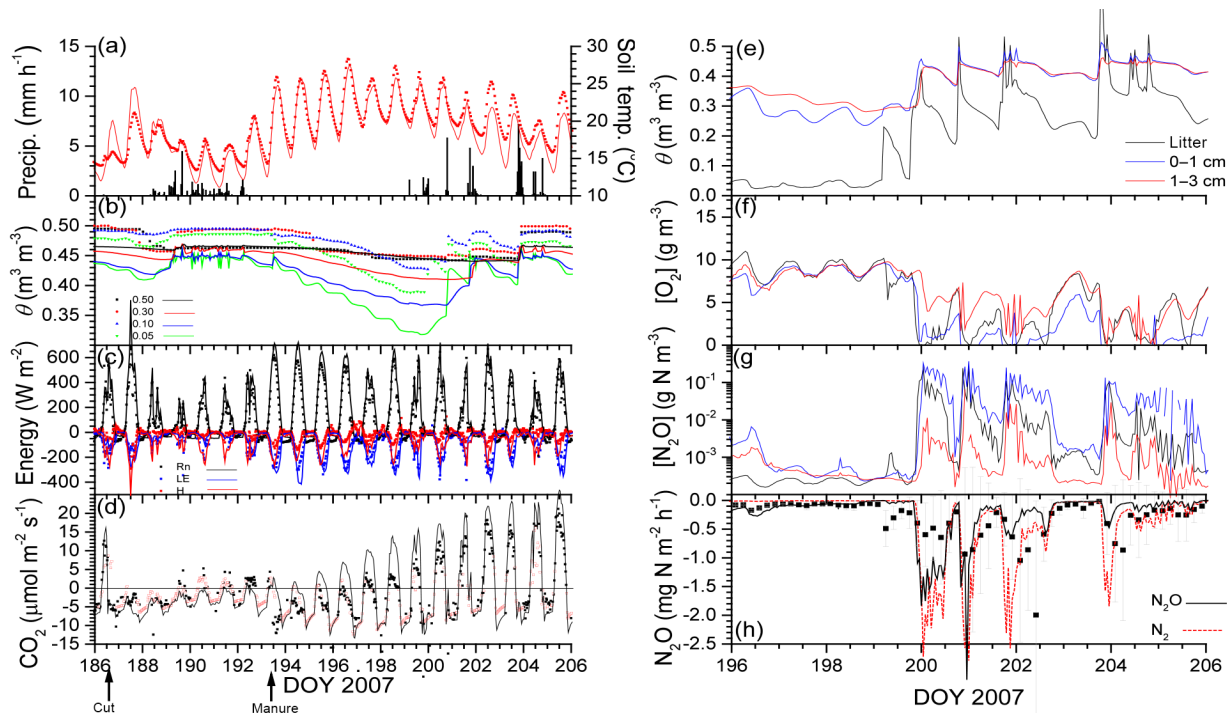


Figure 4. (a) Precipitation and soil temperature at 0.05 m, (b) soil water content (θ) at 0.05, 0.10, 0.30 and 0.50 m, (c) energy, and (d) CO₂ fluxes measured (closed symbols), gap-filled (open symbols) and modelled (lines) during 20 days from harvest (cut) to the end of the emission event following manure application (manure) in July 2007. (e) θ , (f, g) aqueous concentrations of O₂ and N₂O modelled in the surface litter and at 0.01 and 0.02 m in the soil, and (h) N₂O and N₂ fluxes measured (symbols) and modelled (lines) during the last 10 days of this period when the emission event occurred. For fluxes, positive values represent influxes to the soil, negative values effluxes to the atmosphere.

[N₂O_(s)] also drove rises in modelled N₂ emissions (Fig. 5h). Emissions declined with surface litter drying on DOY 223 (Fig. 5e), which allowed surface [O_{2(s)}] to rise (Fig. 5f) and [N₂O_(s)] to fall (Fig. 5g) while θ at 5 cm remained high (Fig. 5b), again indicating that N₂O emissions were largely determined by ecological controls in the surface litter and soil. The net generation of N₂O modelled in each soil zone indicated that 0.48 of surface emissions originated in the surface litter, 0.48 in the 0–1 cm soil layer and 0.05 in the 1–3 cm soil layer, while the deeper soil layers were a very small net sink of N₂O, as indicated by near-surface gradients of [N₂O_(s)] (Fig. 5g).

Greater N₂O emissions were modelled and measured during the event in August 2009 than in July 2007 (Fig. 5h vs. Fig. 4h), in spite of smaller N addition (Fig. 3f vs. Fig. 3d; Table 2) and similar θ and T_s modelled and measured at 5 cm (Fig. 5a, b vs. Fig. 4a, b). These greater emissions were attributed in the model to (1) earlier and heavier precipitation after manure application (2 days after application in Fig. 5a vs. 6 days in Fig. 4a) and (2) slower recovery of CO₂ fixation after defoliation, indicated by slower rises in diurnal amplitude of CO₂ fluxes (Fig. 5d vs. Fig. 4d). Heavier precipitation in 2009 vs. 2007 drove sustained vs. intermittent surface and near-surface wetting (Fig. 5e vs. Fig. 4e) and hence sustained vs. intermittent declines in [O_{2(s)}] and rises

in [N₂O_(s)] (Fig. 5f, g vs. Fig. 4f, g). Slower recovery of CO₂ fixation after cutting in 2009 vs. 2007 slowed removal of added NH₄⁺ and NO₃⁻ from soil. This slower removal, combined with the shorter period between manure application and precipitation, left larger NO₃⁻ concentrations ([NO₃⁻]) in litter and surface soil to drive N₂O production following precipitation [H7]. These model findings indicated the importance to N₂O emissions of surface and near-surface θ after precipitation and of plant management (intensity and timing of defoliation in relation to N application) and its effect on subsequent plant CO₂ fixation and N uptake.

5.5 Effects of intensity and timing of defoliation on N₂O emission events

Increasing harvest intensity and delaying harvest dates slowed LAI regrowth modelled after harvests (Fig. 6). The effects of this slowing on N₂O emissions during selected events modelled after subsequent fertilizer and manure applications were examined under diverse θ and T_s (Figs. 7, 8). Following manure application on DOY 194 in 2006 (Table 2), slower LAI regrowth from increasing and delaying defoliation slowed the recovery of CO₂ fixation (Fig. 7a) and of NH₄⁺ uptake (Fig. 7b), allowing more nitrification of manure N and hence greater surface [NO₃⁻] (Fig. 7c).

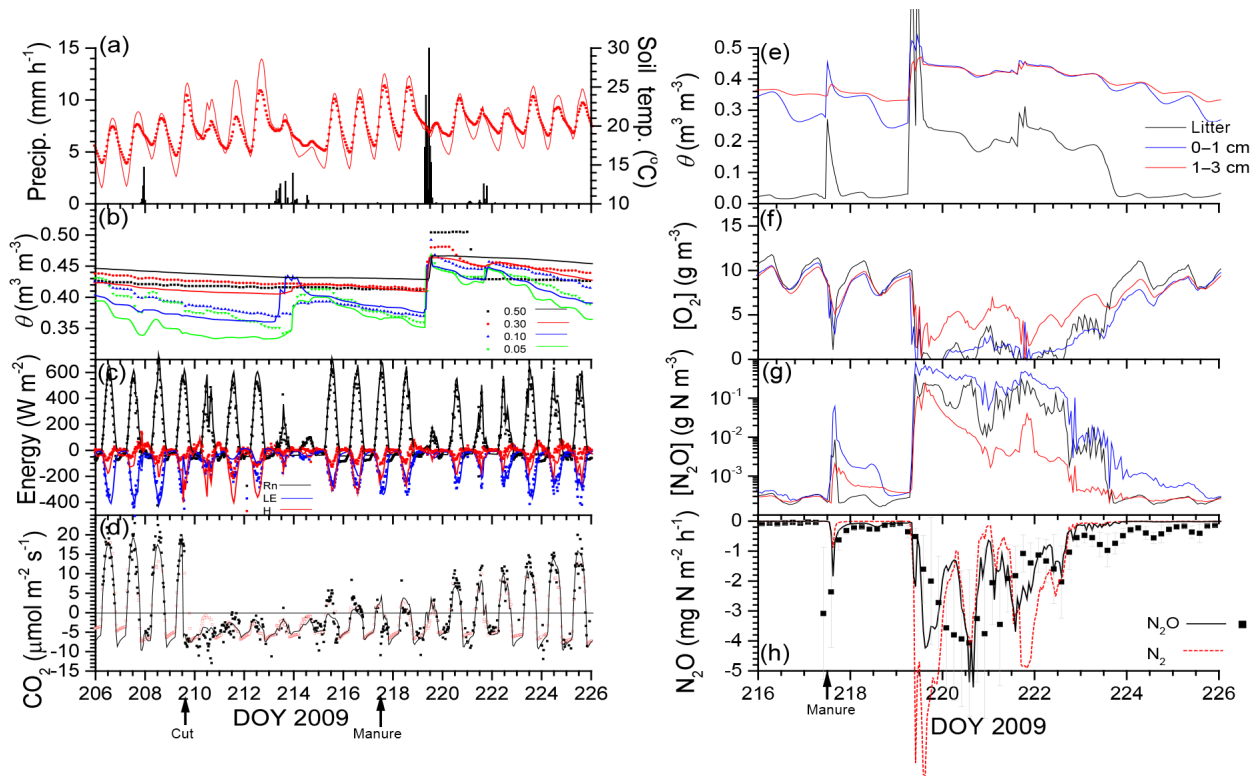


Figure 5. (a) Precipitation and soil temperature at 0.05 m, (b) soil water content (θ) at 0.05, 0.10, 0.30 and 0.50 m, (c) energy, and (d) CO₂ fluxes measured (closed symbols), gap-filled (open symbols) and modelled (lines) during 20 days from harvest (cut) to the end of the emission event following manure application (manure) in August 2008. (e) θ , (f, g) aqueous concentrations of O₂ and N₂O modelled in the surface litter and at 0.01 and 0.02 m in the soil, and (h) N₂O and N₂ fluxes measured (symbols) and modelled (lines) during the last 10 days of this period when the emission event occurred. Positive flux values represent influxes to the soil, negative values effluxes to the atmosphere.

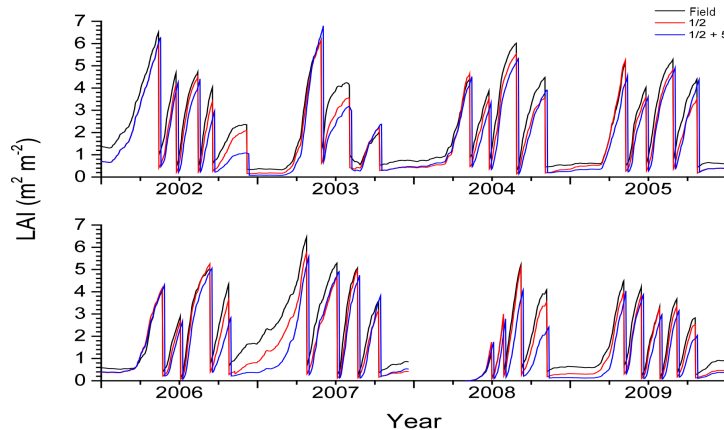


Figure 6. LAI modelled from 2002 through 2009, with LAI after each cut reduced to half of that estimated from the field experiment without or with a delay of 5 days at the Oensingen intensively managed grassland.

Slower LAI regrowth (Fig. 6) also reduced shading and ET, raising T_s (Fig. 7d) and θ (Fig. 7e). N₂O emissions modelled under field management remained small because of soil drying, in spite of high T_s , consistent with measurements (Figs. 3c, 7f). Increases in emissions modelled with slower

LAI regrowth, particularly from delayed harvesting (Fig. 7f), were attributed to slower N uptake (Fig. 7b) and hence larger [NO₃⁻] in litter and surface soil (Fig. 7c) and to warmer and wetter soil (Fig. 7d, e), which increased O₂ demand while reducing O₂ supply.

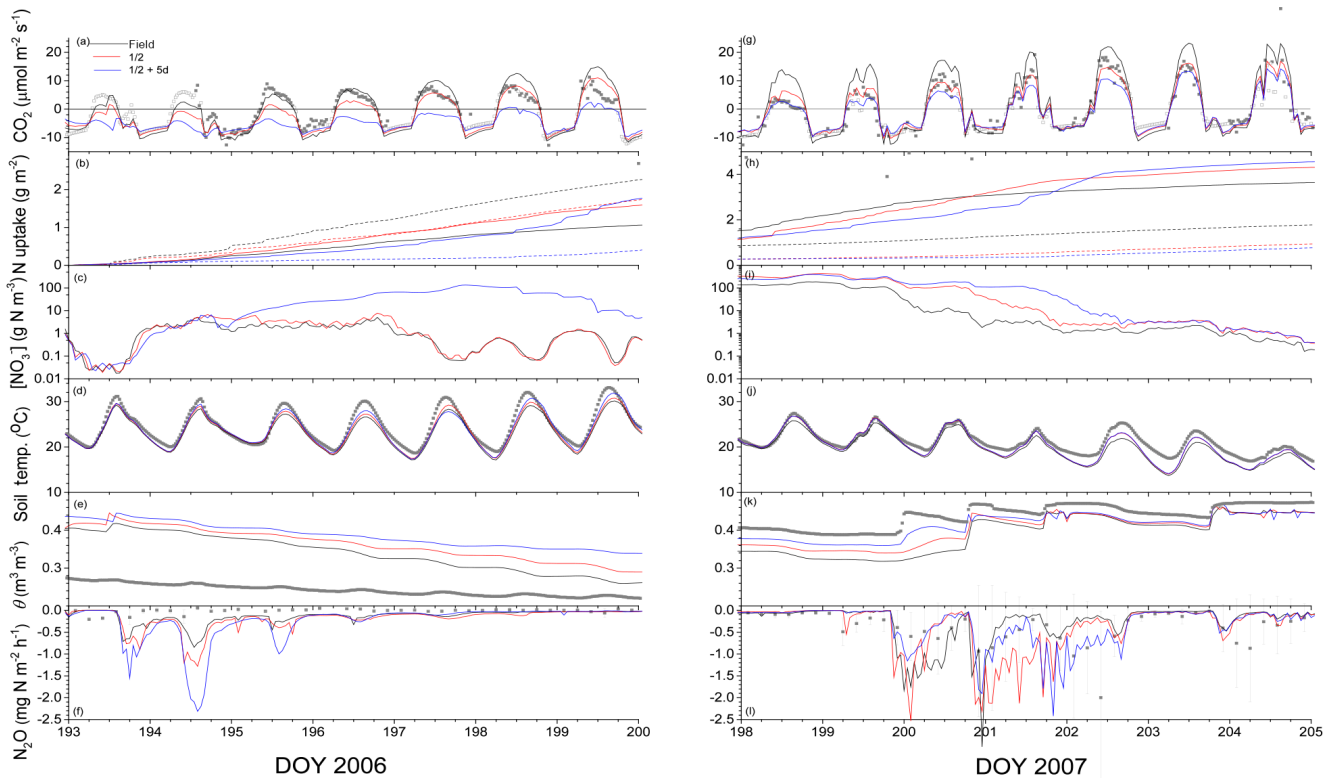


Figure 7. (a, g) CO₂ fluxes, (b, h) cumulative NH₄⁺ (dashed) and NO₃⁻ (solid) uptake since manure application, (c, i) aqueous NO₃⁻ concentrations at 0–1 cm, (d, j) T_s and (e, k) θ at 5 cm, and (f, l) N₂O fluxes measured (symbols) and modelled (lines) with LAI after each cut reduced to half of that estimated from the field experiment without or with a delay of 5 days during emission events following manure applications on DOY 194 in (a–f) 2006 and (g–l) 2007 (see Table 2). For fluxes, positive values represent influxes to the soil, negative values effluxes to the atmosphere.

Following a similar manure application on DOY 194 in 2007 (Table 2; Fig. 6), slower LAI regrowth from increasing and delaying defoliation also caused reductions in CO₂ fixation (Fig. 7g), which slowed NH₄⁺ and NO₃⁻ uptake (Fig. 7h), allowing more nitrification of manure N and hence greater [NO₃⁻] (Fig. 7i). Lower LAI also caused increases in T_s (Fig. 7j) and θ (Fig. 7k). Emissions modelled and measured under field management in 2007 (Fig. 7l) were greater than those in 2006 (Fig. 7f), in spite of lower T_s (Fig. 7j vs. Fig. 7d), because near-surface wetting from several precipitation events (Fig. 4a, e) reduced [O_{2(s)}] and increased [N₂O_(s)] (Fig. 4f, g). Emissions modelled with increased and delayed harvesting rose from those with field harvesting as the emission event progressed (Fig. 7l) because elevated [NO₃⁻] from the manure application persisted longer during the event (Fig. 7i).

Following fertilizer application on DOY 259 in 2005 (Table 2), modelled and measured emissions remained small after soil wetting (Fig. 8f) because lower T_s (Fig. 8d) slowed soil respiration after wetting, manifested as smaller measured and modelled CO₂ effluxes (Fig. 8a), and so slowed demand for e⁻ acceptors. Under these conditions, increasing and delaying defoliation had little effect on modelled N₂O emis-

sions (Fig. 8f), while CO₂ fixation (Fig. 8a) and N uptake (Fig. 8b) were only slightly reduced and surface NO₃⁻ only slightly increased (Fig. 8c). Following the same fertilizer application on DOY 240 in 2007, modelled and measured emissions were greater than those in 2005 (Fig. 8l) because soils were warmer (Fig. 8j) with more rapid respiration (Fig. 8g), and because fertilizer application and subsequent wetting occurred sooner after cutting (Table 2). Consequently, recovery of CO₂ fixation was less advanced (Fig. 8g), reducing cumulative N uptake (Fig. 8h) and leaving larger [NO₃⁻] to drive N₂O generation during the event (Fig. 8h). However, reducing LAI remaining after each harvest did not raise N₂O emissions after this application (Fig. 8l) because slower LAI regrowth from earlier harvests had reduced primary productivity and consequently litterfall and hence the mass of the surface litter from which much of the emitted N₂O was generated. Consequently, more intense harvests could cause surface litter later in the year to decline to levels at which the N₂O generation modelled in the litter was reduced.

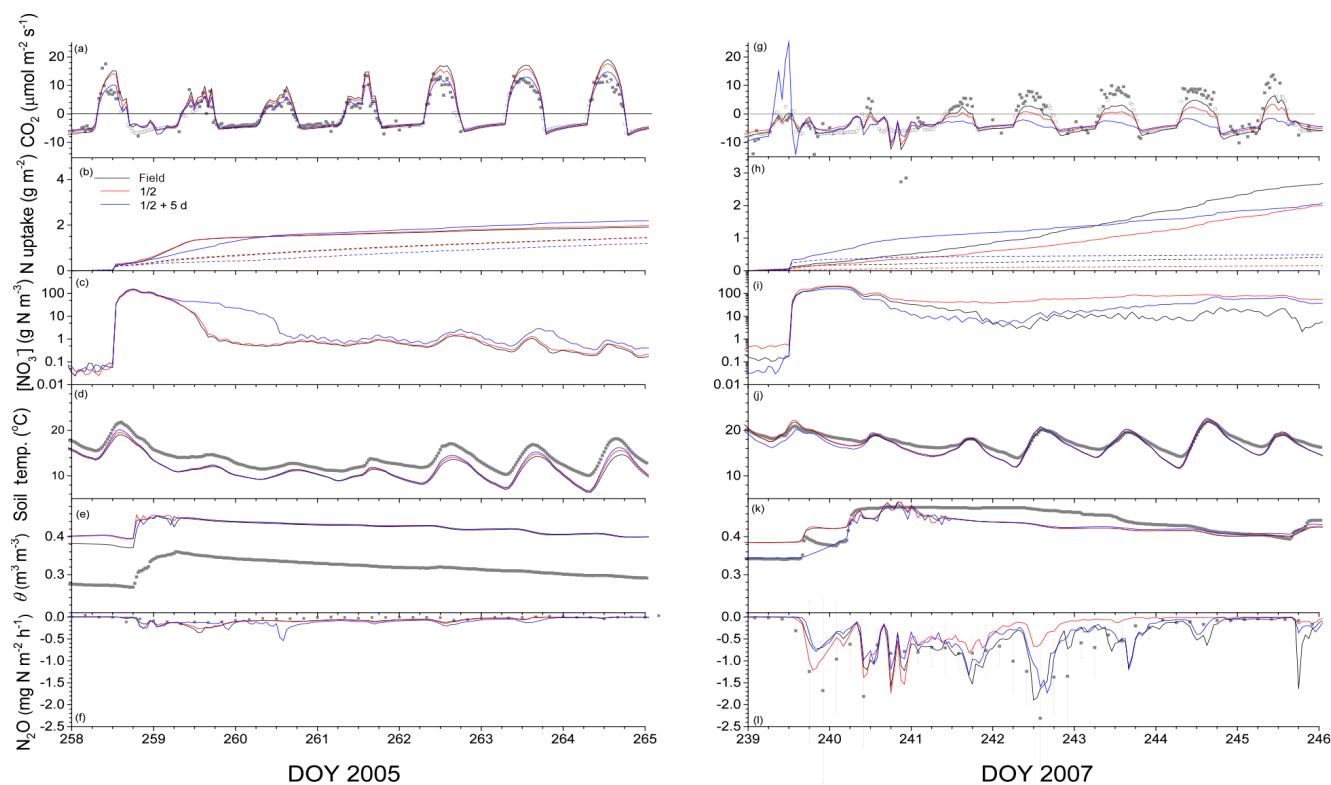


Figure 8. (a, g) CO₂ fluxes, (b, h) cumulative NH₄⁺ (dashed) and NO₃⁻ (solid) uptake since fertilizer application, (c, i) aqueous NO₃⁻ concentrations at 0–1 cm, (d, j) T_s and (e, k) θ at 5 cm, and (f, l) N₂O fluxes measured (symbols) and modelled (lines) with LAI after each cut reduced to half of that estimated from the field experiment without or with a delay of 5 days during emission events following fertilizer applications on DOY 259 in 2005 (a–f) and DOY 240 in 2007 (g–l) (see Table 2). For fluxes, positive values represent influxes to the soil, negative values effluxes to the atmosphere.

5.6 Annual productivity, N₂O emissions, and the effects of defoliation intensity and timing

In the model, plant management practices affected LAI regrowth (Fig. 6), CO₂ fixation, N uptake, and hence soil [NO₃⁻] and N₂O emissions (Figs. 7, 8). These effects were summarized on an annual timescale in Table 4. Modelled and EC-derived gross primary productivity (GPP) remained close to 2000 g C m⁻² yr⁻¹ during most years except with low precipitation in 2003 and replanting in 2008, indicating a highly productive ecosystem with rapid C cycling and hence rapid demand for e⁻ acceptors (Table 4). Larger modelled vs. measured GPP caused larger modelled vs. measured net ecosystem productivity (NEP) in 2003, 2005 and 2007. Harvest removals in the model varied with NEP except during replanting in 2008 but tended to exceed those recorded in the field, particularly with low EC-derived NEP in 2005 and 2006. Modelled values were determined in part by the assumed constant harvest efficiency of 0.76. Including C inputs from manure applications, modelled and estimated net biome productivity (NBP) were positive except during replanting in 2008, indicating that this intensively managed grassland was a C sink unless replanted. Average annual NBP modelled vs.

measured from 2002 to 2009 was 30 vs. 58 g C m⁻², with the lower modelled value attributed to greater modelled harvest removals, particularly in 2006.

Slower LAI regrowth from increasing and delaying defoliation (Fig. 6) reduced modelled GPP, R_e and hence NEP by 5–10 % during years with greater productivity. However, increasing and delaying defoliation did not much affect harvest removals because reduced NEP was offset by greater harvest intensity, so that NBP was reduced except with replanting in 2008.

Annual N₂O emissions were estimated from chamber measurements for each year of the study by scaling the mean measured fluxes to annual values. These values are presented in Table 4 as upper boundaries for annual emissions because flux measurements from which means were calculated were more frequent during emission events. A lower boundary for annual emissions was also estimated in Table 4 by replacing missing flux measurements with zero. Average lower and upper boundaries for annual emissions estimated from 2002 to 2009 were 0.220 and 0.355 g N m⁻² respectively vs. an average annual emission in the model of 0.260 g N m⁻² (Table 4). Modelled emissions were nearer to upper boundaries during years with lower measured emissions (2003, 2004,

Table 4. Annual gross primary productivity (GPP), ecosystem respiration (R_e), net ecosystem productivity (NEP = GPP – R_e), harvest, net biome productivity (NBP) and N₂O emissions derived from EC or chambers and modelled (M) with current land management (Table 2) and with defoliation increased so that LAI remaining after harvesting was reduced by half (1/2), with defoliation increased and delayed by 5 days (1/2 + 5 d). Positive values indicate uptake, negative values emissions.

		Year							
		2002	2003	2004	2005	2006	2007	2008	2009
Precip. (mm)		1478	817	1158	966	1566	1328	1188	1004
MAT (°C)		9.56	9.58	8.92	8.67	9.30	9.59	9.30	9.48
GPP (g C m ⁻² yr ⁻¹)	EC	2159	1773	2058	1766	1817	2102	1455	2119
	M: current	2214	1836	2220	2111	1953	2539	1419	1852
	M: 1/2	2064	1764	2054	1969	1865	2285	1305	1705
	M: 1/2 + 5 d	2014	1774	2076	1966	1771	2277	1225	1686
R_e (g C m ⁻² yr ⁻¹)	EC	-1490	-1558	-1541	-1565	-1577	-1684	-1450	-1657
	M: current	-1560	-1421	-1704	-1679	-1680	-1935	-1366	-1373
	M: 1/2	-1457	-1345	-1569	-1572	-1579	-1714	-1212	-1259
	M: 1/2 + 5 d	-1458	-1350	-1541	-1517	-1519	-1679	-1183	-1235
NEP (g C m ⁻² yr ⁻¹)	EC	669	215	517	201	240	418	5	462
	M: current	654	415	516	432	273	604	53	479
	M: 1/2	607	419	485	397	286	571	93	446
	M: 1/2 + 5 d	556	414	535	449	252	598	42	451
Harvest (g C m ⁻² yr ⁻¹)	field	462	241	401	247	232	448	293	532
	M: current	570	314	525	460	421	690	308	487
	M: 1/2	561	360	465	497	455	678	314	484
	M: 1/2 + 5 d	537	353	579	513	446	686	262	473
C inputs		81	80	29	102	84	160	9	45
NBP (g C m ⁻² yr ⁻¹)	field	288	54	145	56	92	130	-279	-25
	M: current	165	181	20	74	-64	74	-246	37
	M: 1/2	127	139	49	2	-85	53	-212	7
	M: 1/2 + 5 d	101	141	-15	38	-110	72	-211	23
N inputs		27.6	22.5	18.5	24.3	21.4	30.1	9.4	20.0
N ₂ O (g N m ⁻² yr ⁻¹)	chamber								
	upper bound	-0.130	-0.050	-0.060	-0.230	-0.020	-0.280	-0.480	-0.510
	lower bound	-0.450	-0.180	-0.180	-0.320	-0.060	-0.350	-0.620	-0.680
	M: current	-0.302	-0.209	-0.183	-0.193	-0.220	-0.281	-0.326	-0.366
	M: 1/2	-0.269	-0.215	-0.250	-0.249	-0.318	-0.312	-0.335	-0.318
	M: 1/2 + 5 d	-0.284	-0.234	-0.347	-0.352	-0.273	-0.348	-0.327	-0.395

2006) and to lower boundaries during years with higher measured emissions (2007, 2008, 2009). There was no significant correlation between annual N inputs and measured or modelled emissions. Although annual emissions in the model were close to 1 % of annual N inputs during most years, they were greater in 2008 and 2009 in spite of smaller N inputs because of the large emission events modelled after summer applications of fertilizer and manure (Figs. 3e, f, 5h). Annual N inputs (Table 4), supplemented by 3–6 g N m⁻² yr⁻¹ modelled from symbiotic fixation by clover [F1–F26]) were only slightly larger than annual N removals with harvesting, supplemented by losses of 2–3 g N m⁻² yr⁻¹ from all other gaseous and aqueous emissions (N₂ from denitrifica-

tion, NH₃ from volatilization, NO₃⁻ from leaching). Consequently, residual soil NO₃⁻, while present in the model, did not accumulate during the study period, and so did not drive increasing N₂O emissions with sustained N applications. Modelled and measured annual N₂O emissions, if expressed in C equivalents (~130 g C g N⁻¹), largely offset net C uptake expressed as NBP (Table 4).

Increasing harvest intensity and delaying harvest dates had little effect on annual N₂O emissions modelled during the first 2 years after planting in 2001 and 2008 but raised them substantially thereafter (2003–2007) (Table 4). During this period, annual emissions rose by an average of 24 % with

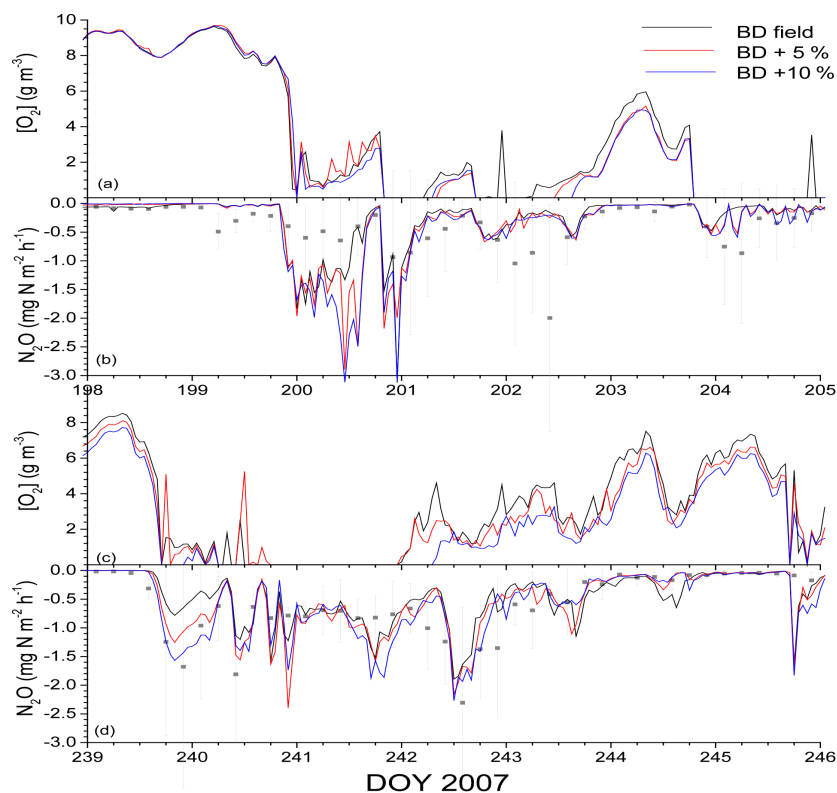


Figure 9. (a, c) Aqueous O₂ concentrations, and (b, d) N₂O fluxes measured (symbols) and modelled (lines) with bulk density (BD) from field measurements and with BD (0–3 cm) raised by 5 or 10 % following (a, b) manure application on DOY 194 and (c, d) fertilizer application on DOY 240 in 2007 (see Table 2). For fluxes, positive values represent influxes to the soil, negative values effluxes to the atmosphere.

increased harvest intensity and by an average of 43 % with increased harvest intensity combined with delayed harvest dates. These increases were attributed to reduced N uptake and to increased T_s and θ (Figs. 7, 8).

5.7 Effects of increased bulk density on N₂O emissions

Increasing near-surface (0–3 cm) soil BD by 5 or 10 % at the beginning of 2001 in the model reduced [O_{2(s)}] after rainfall events and slowed recovery of [O_{2(s)}] during subsequent drying as shown following the manure application in July 2007 (Fig. 9a) and the fertilizer application in late August 2007 (Fig. 9c). These reductions caused increases in modelled N₂O effluxes that varied during emission events (Fig. 9b, d). Effluxes modelled with increases of 10 % in near-surface BD were at times double those modelled without (e.g. DOY 201 and 240 in Fig. 9), indicating that relatively small changes in soil surface properties could at times cause large changes in emissions. The effects of increased BD on modelled T_s , θ , CO₂ exchange, crop production and N uptake during these events were small (results not shown). Increasing near-surface BD by 10 % raised annual N₂O emissions by amounts that increased with annual precipitation from ca. 10 % in drier years (e.g. 2003) to ca. 50 % in wetter years (e.g. 2006) (Table 5).

5.8 Effects of changes in K_{O_2} and K_{NO_x} on N₂O emissions

Lowering K_{O_2} to half that used in *ecosys* reduced annual N₂O emissions modelled from 2004 to 2009 by 16 % to an average of 0.218 g N m⁻² yr⁻¹, near the average lower boundary of the measured values (Table 5). Raising K_{O_2h} to double that used in *ecosys* increased these emissions by 28 % to an average of 0.334 g N m⁻² yr⁻¹, near the average upper boundary of the measured values. Lowering K_{NO_x} to half that used in *ecosys* increased annual N₂O emissions modelled from 2004 to 2009 by 30 % to an average of 0.338 g N m⁻² yr⁻¹, near the average upper boundary of the measured values (Table 5). Raising K_{NO_x} to double that used in *ecosys* reduced these emissions by 27 % to an average of 0.189 g N m⁻² yr⁻¹, near the average lower boundary of the measured values. In years with lower annual emissions (2003, 2004, 2006 in Table 4), the lower K_{O_2} or higher K_{NO_x} gave modelled values that were closer to measured values. However, in years with higher annual emissions (2008 and 2009 in Table 4), the higher K_{O_2} or lower K_{NO_x} gave modelled values that were closer.

Table 5. Annual N₂O emissions modelled with current field management (Table 2) and soil properties (Table 1) (current), with soil bulk density (BD) increased by 5 and 10 % to a depth of 3 cm, and with the Michaelis–Menten constants for reduction of O₂ (K_{O_2}) and of NO₃⁻ and NO₂⁻ (K_{NO_x}) halved or doubled from those used in the model.

		Year							
		2002	2003	2004	2005	2006	2007	2008	2009
Precip. (mm)		1478	817	1158	966	1566	1328	1188	1004
MAT (°C)		9.56	9.58	8.92	8.67	9.30	9.59	9.30	9.48
N ₂ O (g N m ⁻² yr ⁻¹)	current	-0.302	-0.209	-0.183	-0.193	-0.220	-0.281	-0.326	-0.366
	BD + 5 %	-0.352	-0.213	-0.218	-0.199	-0.309	-0.332	-0.358	-0.372
	BD + 10 %	-0.334	-0.235	-0.231	-0.236	-0.336	-0.374	-0.424	-0.371
	$K_{O_2} \times 0.5$	-0.250	-0.179	-0.154	-0.159	-0.160	-0.216	-0.276	-0.349
	$K_{O_2} \times 2.0$	-0.390	-0.263	-0.221	-0.247	-0.315	-0.385	-0.381	-0.468
	$K_{NO_x} \times 0.5$	-0.382	-0.261	-0.265	-0.267	-0.262	-0.378	-0.432	-0.457
$K_{NO_x} \times 2.0$	-0.234	-0.163	-0.126	-0.132	-0.126	-0.208	-0.232	-0.288	

6 Discussion

6.1 Modelled vs. measured N₂O emissions

Most N₂O emission events measured from 2004 to 2009 were simulated within the range of measurement uncertainty, estimated to be about 30 % of mean daily values (Fig. 3). However, some deviations between modelled and measured N₂O emissions were apparent, such as the larger emissions modelled in autumn 2006 (Fig. 3c) and the smaller emissions modelled in spring 2008 (Fig. 3e). These deviations may be attributed to uncertainties in both the measurements and the model. In the automated measurement system, the static chambers were rotated about every 2 months among fixed positions in a corner of the field. During these periods, surface conditions in the chamber could deviate from the mean field conditions represented in the model. However, we do not have an explanation for the very small emissions measured after the three manure slurry applications in 2006. The chambers had been removed before the applications and were reinstalled within 2 h, during which the cut grass was removed so that the surface litter in the chambers may have been reduced from that outside. In the model, emissions following manure or fertilizer applications were sensitive to the amount of surface litter as noted earlier. The absence of emission events measured after slurry applications in 2006 was unusual (Fig. 3) given the large precipitation that year (Table 4), demonstrating that large variability on small spatial scales inevitably affects these measurements. Such variability adversely affects agreement between modelled and measured emissions (Table 3).

During spring 2008 sustained emissions of about 5 mg N m⁻² d⁻¹ were measured by the chambers in the absence of any manure or fertilizer applications (Fig. 3e). These emissions were related to the ploughing of the field to a

depth of 25 cm in December 2007 (Table 2), which hastened soil organic matter decomposition and hence N mineralization that increased mineral N substrate for nitrification and denitrification and possibly for microbial nitrifier and denitrifier populations. These increases must remain conjectural as the Oensingen study did not include a stratified analysis of N₂O production factors (e.g. microbial biomass, potential denitrification) within the chamber soils. Although *ecosys* simulates hastened soil organic matter (SOM) decomposition with tillage (Grant et al., 1998), large amounts of above- and below-ground plant litter with relatively high C : N ratios were incorporated into the model with tillage in December 2007, which slowed net N mineralization and hence accumulation of mineral N products in the model during spring 2008. Consequently, modelled N₂O emissions remained small until mineral N was raised by fertilizer applications in July (Fig. 3c).

6.2 Modelling controls on N₂O emissions by litter and near-surface θ and T_s

In the model, almost all the N₂O emissions originated in the surface litter and in the near-surface (0–1 cm) soil layer, so that emissions were strongly controlled by litter and near-surface θ and T_s (Figs. 3, 4). This model finding is consistent with the experimental finding of Pal et al. (2013) from ¹⁵N enrichment studies that approximately 70 % of N₂O measured during emission events in a managed grassland originated in the surface litter. Similarly van der Weerden et al. (2013) inferred from diurnal variation in T_s and N₂O emissions measured after urine amendments on a managed grassland that N₂O production was at or near the soil surface (0–2 cm). Also Flécharde et al. (2007) inferred in a meta-analysis of N₂O emissions from grasslands in Europe that θ measured at 5 cm was not in some cases an adequate scaling

factor for N₂O source strength because N₂O production and emission took place at or near the soil surface. *Ecosys* simulated little net production, and even a small net consumption, of N₂O in soil below 2 cm during emission events, as may be inferred from peak [N₂O_(s)] modelled in the 0–1 cm soil layer and much lower [N₂O_(s)] modelled in the 1–3 cm soil layer below (Figs. 3g, 4g). This model finding was consistent with the experimental finding of Neftel et al. (2000) that N₂O concentrations below near-surface soil layers in a managed grassland remained below atmospheric values during emission events, from which they inferred that any N₂O generated at depths greater than ~3 cm would not likely reach the soil surface. Thus, attempts to relate N₂O emissions to T_s and θ measured at greater depths than 3 cm in grasslands are unlikely to be informative if these differ from near-surface values. These emissions should rather be related to conditions in the litter and near-surface soil, which need to be better characterized in future studies.

Consequently, modelled N₂O emissions were highly sensitive to surface wetting and drying (e.g. Fig. 4e, h) modelled from precipitation vs. ET (e.g. Fig. 4a, c) or to surface warming and cooling (e.g. Fig. 8j, l) modelled from surface energy balance (e.g. Fig. 4c). The sensitivity to surface wetting and drying was modelled from the effects of θ on air- vs. water-filled porosity and hence on the diffusivity of gases in gaseous [D17] and aqueous [D20] phases and on gaseous volatilization–dissolution transfer coefficients and hence gas exchange between gaseous and aqueous phases [D14, D15]. These transfers controlled O₂ supply, and hence demand for alternative e⁻ acceptors as the O₂ supply fell below O₂ demand, which drove N₂O generation from denitrification [H6–H8] and nitrification [H19]. The control of O₂ supply on e⁻ acceptors used in nitrification thereby simulated the effect of WFPS on the fraction of N₂O generated during nitrification identified by Fang et al. (2015) as necessary to modelling N₂O emissions, while avoiding the model-specific parameterization needed in simpler models. The sensitivity to surface wetting in *ecosys* enabled sharp rises in N₂O emissions to be modelled from surface litter and near-surface soil after small precipitation events during DOY 200–201 in 2007 (Fig. 4a, h) and after slurry application during DOY 218 in 2009 (Fig. 5a, h), even when the soil at 5 cm remained dry (Figs. 4b, 5b). Such rises were consistent with the experimental findings of Flécharde et al. (2007) that precipitation on dry soil can cause substantial N₂O emissions after fertilizer application in grasslands.

The sensitivity to surface warming and cooling was modelled from the effects of T_s on the diffusivity of gases in gaseous [D17] and aqueous [D20] phases and on the solubility of gases and hence the exchange of gases between gaseous and aqueous phases [D14, D15], both parameterized from basic physical relationships independently of the model. These transfers controlled [O_{2(s)}] in the surface litter and soil (Figs. 3f, 4f) and hence O₂ uptake by aerobic heterotrophs [H4] and autotrophs [H13] through a Michaelis–

Menten constant [H4b, H13b]. The sensitivity to surface warming and cooling was also modelled from the effects of T_s on soil organic carbon (SOC) oxidation [H2] and hence O₂ demand by aerobic heterotrophs [H3] and on NH₄⁺ and NO₂⁻ oxidation [H11, H15] and hence O₂ demand by aerobic autotrophs [H12, H16]. These effects were driven by a single Arrhenius function used for all biological transformations [A6] parameterized from basic research conducted independently of the model. Under sustained high surface θ , this combination of physical and biological processes drove large diurnal variation in N₂O emissions modelled with diurnal surface warming and cooling during emission events (e.g. DOY 221 in Fig. 5h, DOY 243 in Fig. 8l), as observed experimentally by van der Weerden et al. (2013). By explicitly simulating the diverse processes that determine N₂O emissions, *ecosys* could model the large sensitivity of emissions to T_s without the use of unrealistically large parameters for temperature sensitivity inferred from controlled temperature studies of N₂O emissions (e.g. Dobbie and Smith, 2001). This large sensitivity to T_s has been inadequately represented in simpler models, causing the underestimation of large emissions measured from warm soils (e.g. Saggart et al., 2004). On a seasonal timescale higher T_s could cause large increases in N₂O emissions modelled with comparable θ after the same fertilizer application (Fig. 8l vs. Fig. 8f). However, the effects of T_s on N₂O emissions were dominated by those of θ during surface wetting and drying (e.g. Figs. 4h, 7l).

Values of both θ and T_s thus determined O₂ demand not met by O₂ uptake, which drove demand for alternative e⁻ acceptors by heterotrophic denitrifiers [H6] and autotrophic nitrifiers [H19]. This demand drove the sequential reduction of NO₃⁻, NO₂⁻ and N₂O to NO₂⁻, N₂O and N₂ respectively by heterotrophic denitrifiers [H7, H8, H9] and the reduction of NO₂⁻ to N₂O by autotrophic nitrifiers [H20]. The consequent production of N₂O (Figs. 4g, 5g) and N₂ drove emissions of both N₂O and N₂ (Figs. 4h, 5h) through volatilization [D14, D15] and through gaseous and aqueous diffusion [D16, D19]. Ratios of N₂O and N₂ emissions in *ecosys* (Fig. 4h, 5h) were not parameterized as done in other models but rather were determined by relative affinities determined from basic research [H8, H9] and by environmental conditions. When demand from heterotrophic denitrifiers for alternative e⁻ acceptors was small relative to their availability, the preferential reduction of more oxidized e⁻ acceptors generated larger emissions of N₂O [H7, H8] relative to N₂ [H9]. Such conditions occurred during the early part of an emission event when surface [NO₃⁻] rose with nitrification of fertilizer or manure NH₄⁺ after application (e.g. DOY 200–201 in Fig. 4h). However, when demand for alternative e⁻ acceptors was large relative to their availability, this same reduction sequence forced a more rapid reduction of N₂O to N₂ and hence smaller emissions of N₂O relative to N₂. Such conditions occurred during the later part of emission

events when surface [NO₃⁻] declined with plant uptake (e.g. DOY 202–205 in Fig. 4h and DOY 222 in Fig. 5h) or when greater surface wetting reduced O₂ supply (e.g. DOY 220 in Fig. 5h). This greater demand for alternative e⁻ acceptors with wetting provided a process-based explanation for declines in N₂O emissions frequently found at higher θ in field studies (e.g. Rafique et al., 2011) without explicit parameterization of N₂O : N₂ ratios.

Nitrification and denitrification were also driven by the concentrations of NH₄⁺ [H11], NO₃⁻ [H7], NO₂⁻ [H8, H15, H20] and N₂O [H9] relative to Michaelis–Menten constants evaluated from basic research. The concentrations of NH₄⁺ and NO₃⁻ in *ecosys* were increased by N additions from manure and fertilizer N applications (Table 2) and by net mineralization soil organic N from oxidation of litterfall, manure and SOM [A26] as indicated by soil CO₂ effluxes. These concentrations were reduced by root uptake of NH₄⁺ and NO₃⁻ [C23] and consequent plant N assimilation with growth, indicated by more rapid CO₂ fixation with time after cutting (Figs. 3, 4, 6, 7). In the model, more rapid CO₂ fixation drove a more rapid production of nonstructural C, and hence a more rapid exchange of nonstructural C and N between canopy and roots [C50], and so hastened root active N uptake by increasing R_a driving root growth [C14b] and by hastening the removal of N uptake products and hence reducing their inhibition of active uptake [C23g]. The diversity of controls on key substrates for N₂O generation suggests that robust simulations of N₂O emissions require comprehensive ecosystem models in which these controls are fully represented.

6.3 Modelling effects of defoliation intensity and timing on N₂O emissions

The control of NH₄⁺ and NO₃⁻ availability by root N uptake indicated that plant management practices determining uptake would thereby affect N₂O emissions. In the model, increasing harvest intensity and delaying harvest dates both slowed N uptake (Figs. 7b, h, 8b, h) by slowing the recovery of LAI (Fig. 6) and CO₂ fixation (Figs. 7a, g, 8a, g). Both thereby increased [NO₃⁻] (Figs. 7c, i, 8c, i), T_s (Figs. 7d, j, 8d, j) and θ (Figs. 7e, k, 8e, k), raising N₂O effluxes modelled during most emission events (Figs. 7f, l, 8f, l) and hence annually (Table 4). This model finding was consistent with the field observations of Jackson et al. (2015) that increased N₂O emissions after defoliation in grasslands were caused by the reduced uptake of N and water by slower-growing plants.

The effects of defoliation on N₂O emissions during modelled emission events were similar to, or greater than, those of T_s and θ (e.g. Fig. 7f, l), consistent with the experimental finding of Imer et al. (2013) that plant management, as represented by its effects on LAI, had a larger effect on N₂O fluxes than did the environment, as represented by T_a , at an intensively managed grassland in Switzerland. Reducing LAI remaining after harvest by half and delaying harvest by

5 days had little effect on modelled harvest removals (Table 4), suggesting that N₂O emissions from managed grasslands are more sensitive to plant management practices than are yields. The intensity and timing of harvests should therefore be selected to avoid slow regrowth of LAI following N additions by avoiding excessive defoliation and by allowing as much time as possible between defoliation and subsequent fertilizer or manure application. Neftel et al. (2010) reported enhanced N₂O emissions after cuts in managed grassland and hypothesized that a simple mitigation option would be to optimize the timing of the fertilizer applications. To our knowledge this option has not been systematically investigated.

6.4 Modelling effects of soil bulk density on N₂O emissions

The small increases in near-surface BD included in this study were typical of those arising from natural variation in soil properties or from compaction by vehicular traffic during field management operations. In the model, these increases reduced soil porosity and hence gaseous diffusivity [D17] which slowed O₂ uptake from the atmosphere [D15] and O₂ transfer through the soil profile [D16]. Consequent reductions in near-surface [O_{2(s)}] (Fig. 9a, c) slowed O₂ reduction by denitrifiers [H4] and nitrifiers [H13], forcing more rapid e⁻ transfer to NO₃⁻ by denitrifiers [H6] and to NO₂⁻ by nitrifiers [H19] and hence more rapid emissions of N₂O following applications of manure (Fig. 9b) and fertilizer (Fig. 9d).

In a study of soil compaction effects on N₂O emissions from a fertilized agricultural field in a climate similar to that at Oensingen, Bessou et al. (2010) found that increasing the BD of the upper 30 cm of the soil profile by ca. 15 % raised annual N₂O emissions measured with automated chambers by at least 50 % during each of two growing seasons. These rises were similar to those modelled with a smaller increase in BD of the upper 3 cm during the wettest year of this study (Table 5). During emission events, Bessou et al. (2010) measured peak fluxes from compacted soil that were double those from uncompacted, as also modelled here (Fig. 9b, d).

The detailed algorithms from which *ecosys* was constructed enabled increases in N₂O emissions from surface compaction to be simulated from specified changes to surface BD, a measurable site characteristic, without further model parameterization. The marked increases in N₂O emissions modelled with these increases in BD (Table 5) indicated that some of the large spatial variation in these emissions commonly found in field measurements could arise from relatively small variation in physical properties of near-surface soil. In future studies of N₂O emissions, near-surface soil properties could be determined at each measurement site to establish the extent to which variation in these properties is associated with those in emissions.

6.5 Modelling effects of K_{O_2} and K_{NO_x} on N₂O emissions

The value of K_{O_2} used in *ecosys* ($= 2 \mu\text{M}$) was taken from the upper range of values determined experimentally for intact cells of heterotrophic bacteria by Longmuir (1954). Halving or doubling K_{O_2} changed modelled N₂O emissions (Table 5) by amounts similar to uncertainty in measured emissions expressed as lower and upper boundaries of likely values (Table 4), although the doubled value of K_{O_2} was larger than those derived from experiments. The value of K_{NO_x} used in *ecosys* ($= 100 \mu\text{M}$) was within the range of values determined experimentally by Yoshinari et al. (1977). As for K_{O_2} , halving or doubling K_{NO_x} changed modelled N₂O emissions (Table 5) by amounts similar to uncertainty in measured emissions expressed as lower and upper boundaries of likely values (Table 4). The halved value of K_{NO_x} was closer to those measured by Betlach and Tiedje (1981) and Khalil et al. (2005), while the doubled value was closer to that measured by Klemedtsson et al. (1977). These changes indicate that key parameters used in process models must be capable of being constrained by accurate evaluation in independent experiments.

7 Conclusions

N₂O emissions modelled in this managed grassland originated in the surface litter and upper 2 cm of the soil profile. The shallow origin of these emissions enabled *ecosys* to simulate the response of measured emissions to changes in near-surface θ and T_s during brief emission events when rainfall followed manure or mineral fertilizer applications. Measurements of θ and T_s used to estimate N₂O emissions from managed grasslands should therefore be taken in surface litter and near-surface soil (0–2 cm), rather than deeper in the soil profile (5–10 cm) as is currently done.

N₂O fluxes modelled during emission events were greater when grassland regrowth and hence mineral N uptake was slower following harvest and subsequent N application. The control of N₂O emissions by grassland N uptake indicated that N₂O emissions from managed grassland could be increased by harvesting practices and fertilizer timing that resulted in slower regrowth during periods when emission events are most likely to occur. N₂O fluxes modelled during emission events rose sharply with small increases in surface BD, indicating the importance of avoiding surface compaction in fields to which large amounts of N are applied.

The basic and comprehensive approach to model development in *ecosys* allowed diverse responses of N₂O emissions to changes in weather (T_s , θ), land management and soil properties to be modelled from specified changes to readily measured inputs with parameters constrained by basic experiments conducted independently of the model rather than derived from site-specific observations. This approach

enabled concurrent, well-constrained tests of model performance against a diverse set of field measurements and so is expected to confer robustness to the modelling of these emissions under different climates, soils and land uses in future studies.

The Supplement related to this article is available online at doi:10.5194/bg-13-3549-2016-supplement.

Acknowledgements. Computational facilities for *ecosys* were provided by the University of Alberta and by the Compute Canada high-performance computing infrastructure. A PC version of *ecosys* with GUI can be obtained by contacting the corresponding author at rgrant@ualberta.ca. The authors also acknowledge contributions from valuable discussions with Christoph Amman concerning measurement methodology.

Edited by: A. Ibrom

References

- Ammann, C., Fléchar, C., Leifeld, J., Neftel, A., and Fuhrer, J.: The carbon budget of newly established temperate grassland depends on management intensity, *Agr. Ecosyst. Environ.*, 121, 5–20, 2007.
- Ammann, C., Spirig, C., Leifeld, J., and Neftel, A.: Assessment of the nitrogen and carbon budget of two managed temperate grassland fields, *Agr. Ecosyst. Environ.*, 133, 150–162, 2009.
- Bessou, C., Mary, B., Léonard, J., Roussel, M., Gréhan, E., and Gabrielle, B.: Modelling soil compaction impacts on nitrous oxide emissions in arable fields, *Eur. J. Soil Sci.*, 61, 348–363, 2010.
- Betlach, M. R. and Tiedje, J. M.: Kinetic explanation for accumulation of nitrite, nitric oxide, and nitrous oxide during bacterial denitrification. *Appl. Environ. Microb.*, 42, 1074–1084, 1981.
- Chatskikh, D. D., Olesen, J. E., Berntsen, J., Regina, K., and Yamilki, S.: Simulation of effects of soils, climate and management on N₂O emission from grasslands, *Biogeochemistry*, 76, 395–419, 2005.
- Conant, R. T., Paustian, K., Del Grosso, S. J., and Parton, W. J.: Nitrogen pools and fluxes in grassland soils sequestering carbon, *Nutr. Cycl. Agroecosys.*, 71, 239–248, 2005.
- Craswell, E. T.: Some factors influencing denitrification and nitrogen immobilization in a clay soil, *Soil Biol. Biochem.*, 10, 241–245, 1978.
- Dobbie, K. E. and Smith, K. A.: The effect of temperature, water-filled pore space, and land use on N₂O emissions from an imperfectly drained gleysol, *Eur. J. Soil Sci.*, 52, 667–673, 2001.
- Fang, Q. X., Ma, L., Halvorson, A. D., Malone, R. W., Ahuja, L. R., Del Grosso, S. J., and Hatfield, J. L.: Evaluating four nitrous oxide emission algorithms in response to N rate on an irrigated corn field, *Environ. Modell. Softw.*, 72, 56–70, 2015.

- Felber, R., Leifeld, J., Horak, J., and Neftel, A.: Nitrous oxide emission reduction with greenwaste biochar: comparison of laboratory and field experiments, *Eur. J. Soil Sci.*, 65, 128–138, doi:10.1111/ejss.12093, 2014.
- Fléclard, C. R., Neftel, A., Jocher, M., Ammann, C., and Fuhrer, J.: Bi-directional soil/atmosphere N₂O exchange over two mown grassland systems with contrasting management practices, *Glob. Change Biol.*, 11, 2114–2127, 2005.
- Fléclard, C. R., Ambus, P., Skiba, U., et al.: Effects of climate and management intensity on nitrous oxide emissions in grassland systems across Europe, *Agr. Ecosyst. Environ.*, 121, 135–152, 2007.
- Grant, R. F.: A Review of the Canadian Ecosystem Model – *ecosys*, chapter 6, in: *Modeling Carbon and Nitrogen Dynamics for Soil Management*, edited by: Shaffer, M., CRC Press, Boca Raton, FL, USA, 173–264, 2001.
- Grant, R. F. and Pattey, E.: Mathematical modelling of nitrous oxide emissions from an agricultural field during spring thaw, *Global Biogeochem. Cy.*, 13, 679–694, 1999.
- Grant, R. F. and Pattey E.: Modelling variability in N₂O emissions from fertilized agricultural fields, *Soil Biol. Biochem.*, 35, 225–243, 2003.
- Grant, R. F. and Pattey, E.: Temperature sensitivity of N₂O emissions from fertilized agricultural soils: mathematical modelling in *ecosys*, *Global Biogeochem. Cy.*, 22, GB4019, doi:10.1029/2008GB003273, 2008.
- Grant, R. F., Juma, N. G., and McGill, W. B.: Simulation of carbon and nitrogen transformations in soils. I. Mineralization, *Soil Biol. Biochem.*, 27, 1317–1329, 1993a.
- Grant, R. F., Juma, N. G., and McGill, W. B.: Simulation of carbon and nitrogen transformations in soils. II. Microbial biomass and metabolic products, *Soil Biol. Biochem.*, 27, 1331–1338, 1993b.
- Grant, R. F., Izaurrealde, R. C., Nyborg, M., Malhi, S. S., Solberg, E. D., and Jans-Hammermeister, D.: Modelling tillage and surface residue effects on soil C storage under current vs. elevated CO₂ and temperature in *ecosys*, in: *Soil processes and the carbon cycle*, edited by: Lal, R., Kimble, J. M., Follet, R. F., and Stewart, B. A., CRC Press, Boca Raton, FL, 527–547, 1998.
- Grant, R. F., Pattey, E. M., Goddard, T. W., Kryzanowski, L. M., and Puurveen, H.: Modelling the effects of fertilizer application rate on nitrous oxide emissions from agricultural fields, *Soil Sci. Soc. Am. J.*, 70, 235–248, 2006.
- Grant, R. F., Baldocchi, D. D., and Ma, S.: Ecological controls on net ecosystem productivity of a Mediterranean grassland under current and future climates, *Agr. Forest Meteorol.*, 152, 189–200, 2012.
- Imer, D., Merbold, L., Eugster, W., and Buchmann, N.: Temporal and spatial variations of soil CO₂, CH₄ and N₂O fluxes at three differently managed grasslands, *Biogeosciences*, 10, 5931–5945, doi:10.5194/bg-10-5931-2013, 2013.
- Jackson, R. D., Oates, L. G., Schacht, W. H., Klopfenstein, T. J., Undersander, D. J., Greenquist, M. A., Bell, M. M., and Gratton, C.: Nitrous oxide emissions from cool-season pastures under managed grazing, *Nutr. Cycl. Agroecosys.*, 101, 365–376, 2015.
- Khalil, K., Renault, P., Guérin, N., and Mary, B.: Modelling denitrification including the dynamics of denitrifiers and their progressive ability to reduce nitrous oxide: comparison with batch experiments, *Eur. J. Soil Sci.*, 56, 491–504, 2005.
- Klemetsson, L., Svensson, B. H., Lindberg, T., and Rosswall, T.: The use of acetylene inhibition of nitrous oxide reductase in quantifying denitrification in soils, *Swed. J. Agri. Res.*, 7, 179–185, 1977.
- Leifeld, J., Ammann, C., Neftel, A., and Fuhrer, J.: A comparison of repeated soil inventory and carbon flux budget to detect soil carbon changes after conversion from cropland to grasslands, *Glob. Change Biol.*, 17, 3366–3375, 2011.
- Li, Y., Chen, D., Zhang, Y., Edis, R., and Ding, H.: Comparison of three modeling approaches for simulating denitrification and nitrous oxide emissions from loam-textured arable soils, *Global Biogeochem. Cy.*, 19, GB3002, doi:10.1029/2004GB002392, 2005.
- Longmuir, I. S.: Respiration rate of bacteria as a function of oxygen concentration, *Biochem. J.*, 51, 81–87, 1954.
- Lu, Y., Huang, Y., Zou, J., and Zheng, X.: An inventory of N₂O emissions from agriculture in China using precipitation-rectified emission factor and background emission, *Chemosphere*, 65, 1915–1924, 2006.
- Metivier, K. A., Pattey, E., and Grant, R. F.: Using the *ecosys* mathematical model to simulate temporal variability of nitrous oxide emissions from a fertilized agricultural soil, *Soil Biol. Biochem.*, 41, 2370–2386, 2009.
- Neftel, A., Blatter, A., Schmid, M., Lehmann, B., and Tarakanov, S. V.: An experimental determination of the scale length of N₂O in the soil of a grassland, *J. Geophys. Res.*, 105, 12095–12103, 2000.
- Neftel, A., Spirig, C., and Ammann, C.: Application and test of a simple tool for operational footprint evaluations, *Environ. Pollut.*, 152, 644–652, 2008.
- Neftel, A., Ammann, C., Fischer, F., Spirig, C., Conen, F., Emmenegger, L., Tuzson, B., and Wahlen, S.: N₂O exchange over managed grassland: Application of a quantum cascade laser spectrometer for micrometeorological flux measurements, *Agr. Forest Meteorol.*, 150, 775–785, 2010.
- Pal, P., Clough, T. J., Kelliher, F. M., and Sherlock, R. R.: Nitrous oxide emissions from in situ deposition of 15N-labeled ryegrass litter in a pasture soil, *J. Environ. Qual.*, 42, 323–331, 2013.
- Pedersen, A. R., Petersen, S. O., and Schelde, K.: A comprehensive approach to soil-atmosphere trace-gas flux estimation with static chambers, *Eur. J. Soil Sci.*, 61, 888–902, 2010.
- Rafique, R., Hennessy, D., and Kiely, G.: Nitrous oxide emission from grazed grassland under different management systems, *Ecosystems*, 14, 563–582, 2011.
- Ruzjerez, B. E., White, R. E., and Ball, P. R.: Long-term measurement of denitrification in three contrasting pastures grazed by sheep, *Soil Biol. Biochem.*, 26, 29–39, 1994.
- Saggar, S., Andrew, R. M., Tate, K. R., Hedley, C. B., Rodda, N. J., and Townsend, J. A.: Modelling nitrous oxide emissions from dairy-grazed pastures, *Nutr. Cycl. Agroecosys.*, 68, 243–255, 2004.
- Saxton, K. E. and Rawls, W. J.: Soil water characteristic estimates by texture and organic matter for hydrologic solutions, *Soil Sci. Soc. Am. J.*, 70, 1569–1578, 2006.
- Saxton, K. E., Rawls, W. J., Romberger, J. S., and Papendick, R. I.: Estimating generalized soil-water characteristics from texture, *Soil Sci. Soc. Am. J.*, 50, 1031–1036, 1986.

- Schmid, M., Neftel, A., Riedo, M., and Fuhrer, J.: Process-based modelling of nitrous oxide emissions from different nitrogen sources in mown grassland, *Nutr. Cycl. Agroecosys.*, 60, 177–187, 2001.
- Smith, K. A. and Massheder, J.: Predicting nitrous oxide emissions from N-fertilized grassland soils in the UK from three soil variables, using the B-LINE 2 model, *Nutr. Cycl. Agroecosys.*, 98, 309–326, 2014.
- van der Weerden, T. J., Clough, T. J., and Styles, T. M.: Using near-continuous measurements of N₂O emission from urine-affected soil to guide manual gas sampling regimes, *New Zeal. J. Agr. Res.*, 56, 60–76, 2013.
- Yoshinari, T., Hynes, R., and Knowles, R.: Acetylene inhibition of nitrous oxide reduction and measurement of denitrification and nitrogen fixation in soil, *Soil Biol. Biochem.*, 9, 177–183, 1977.